BRNO UNIVERSITY OF TECHNOLOGY
VYSOKÉ UČENÍ TECHNICKÉ V BRNĚ

FACULTY OF MECHANICAL ENGINEERING
FAKULTA STROJNÍHO INŽENÝRSTVÍ

INSTITUTE OF MATHEMATICS
ÚSTAV MATEMATIKY

STABILITY AND CHAOS IN NONLINEAR DYNAMICAL SYSTEMS
STABILITA A CHAOS V NELINEÁRNÍCH DYNAMICKÝCH SYSTÉMECH

MASTER'S THESIS
DIPLOMOVÁ PRÁCE

AUTHOR
AUTOR PRÁCE
      Bc. Jitka Khůlová

SUPERVISOR
VEDOUCÍ PRÁCE
      doc. RNDr. Jan Čermák, CSc.

BRNO 2018

Specification Master's Thesis

Department:	Institute of Mathematics
Student:	**Bc. Jitka Khůlová**
Study programme:	Applied Sciences in Engineering
Study branch:	Mathematical Engineering
Leader:	**doc. RNDr. Jan Čermák, CSc.**
Academic year:	2017/18

Pursuant to Act no. 111/1998 concerning universities and the BUT study and examination rules, you have been assigned the following topic by the institute director Master's Thesis:

Stability and chaos in nonlinear dynamical systems

Concise characteristic of the task:

Stability and chaos belong among the most important characteristics of nonlinear dynamical systems. Transition from stability to chaotic behaviour was first desribed in the study of the Lorenz dynamical model of conventional fluid in atmosphere. Recently, some other deterministic models displaying chaotic behaviour have appeared. Stabilization and synchronization of these systems belong among the main research topics.

Goals Master's Thesis:

1. A survey of basic dynamical systems with chaotic behaviour.
2. Analysis of a given model and its transition from stable to chaotic behaviour.
3. Stabilization and synchronization of dynamical systems.
4. Numerical experiments and graphical simulations.

Recommended bibliography:

HÖVEL, P. Control of Complex Nonlinear Systems with Delay. Springer, 2010. ISBN 978-3-6-2-14109-6.

STROGATZ, S.H. Nonlinear Dynamics and Chaos: With Applications to Physics, Biology, Chemistry and Engineering. Reading: Perseus Books, 1994. ISBN 0-201-54344-3.

Deadline for submission Master's Thesis is given by the Schedule of the Academic year 2017/18

In Brno,

L. S.

....
prof. RNDr. Josef Šlapal, CSc.   doc. Ing. Jaroslav Katolický, Ph.D.
Director of the Institute   FME dean

Deadline for submission Master's Thesis is given by the Schedule of the Academic year 2017/18

In Brno,

ABSTRACT

The master's thesis deals with analysis of basic chaotic dynamical systems, with a special emphasis put on the Rössler system. Besides standard bifurcation analysis, stabilization problems related to this system are investigated. The diagonal time-delayed feedback control is utilized as a basic control tool for this problem. Using derived theoretical results, optimal conditions for control gain and time delay parameters are established. In addition, a synchronization problem for two Rössler systems is discussed and investigated for several synchronization methods.

KEYWORDS

Chaotic dynamical system, Rössler system, bifurcation analysis, stabilization, time-delayed feedback control, synchronization

ABSTRAKT

Diplomová práce pojednává o teorii chaotických dynamických systémů, speciálně se pak zabývá Rösslerovým systémem. Kromě standardních výpočtů spojených s bifurkační analýzou se práce zaměřuje na problém stabilizace, konkrétně na stabilizaci rovnovážných bodů. Ke stabilizaci je využita základní metoda zpětnovazebního řízení s časovým zpožděním. Významnou část práce tvoří zavedení a implementace obecné metody pro hledání vhodné volby parametrů vedoucí k úspěšné stabiliaci. Dalším diskutovaným tématem je možnost synchronizace dvou Rösslerových systémů pomocí různých synchronizačních schémat.

KLÍČOVÁ SLOVA

Chaotické dynamické systémy, Rösslerův systém, bifurkační analýza, stabilizace, časově zpožděné zpětnovazební řízení, synchronizace

ROZŠÍŘENÝ ABSTRAKT

Chaotické dynamické systémy tvoří významnou část v teorii dynamických systémů. Jedná se o systémy, které vykazují velkou citlivost na volbu počátečních podmínek. Jinými slovy systémy, u kterých se vývoj dvou velmi blízkých počátečních bodů značně rozchází s rostoucím časem. V případě systémů se spojitým časem, tj. systémů popsaných soustavou obyčejných diferenciálních rovnic, se chaos objevuje u nelineárních systémů alespoň dimenze 3. Chaos byl v minulosti považován za nežádoucí jev a nebyla mu věnována příliš velká pozornost. Éra chaosu započala v roce 1963 objevem Lorenzova podivného atraktoru. Lorenzův systém popisuje zjednodušený model nucené konvekce v atmosféře. Studováním daného modelu, Lorenz objevil souvislost mezi chaotickými systémy a fraktálními strukturami. Ukázal, že i přes zdánlivě nahodilé a nepředvídatelné chování, systém zůstává ohraničený v určité oblasti, která byla později nazvána podivný atraktor. Lorenzův systém, který jistě patří mezi nejznámější systémy, je také proslulý pod názvem "The Butterfly Effect".

Předložená diplomová práce se zabývá známými chaotickými systémy, jejichž výčet, stručný popis a volba charakteristických parametrů jsou uvedeny ve 2. kapitole. Kromě nejznámějších systémů, jako je Lorenzův nebo Rösslerův model, se v této kapitole objevují další chaotické systémy, které byly objeveny v různých vědních oborech. Příkladem je Bělousovova–Žabotinského chemická reakce, Chuův elektrický obvod nebo modifikovaný Van der Pollův oscilátor. Tyto modely jsou pro lepší ilustraci doplněny charakteristickými fázovými portréty.

V dalších kapitolách je práce zaměřena převážně na případ Rösslerova chaotického modelu, který je dán soustavou 3 diferenciálních rovnic s jedním nelineárním členem

$$
\begin{aligned}
x' &= -y - z\,,\\
y' &= x + ay\,,\\
z' &= b + z(x - c)\,,
\end{aligned}
$$

kde $a\,,b\,,c$ jsou reálné parametry.

3. kapitola se detailně zabývá analýzou stability rovnovážných bodů a bifurkační analýzou Rösslerova systému s využitím teoretických předpokladů uvedených v 1. kapitole. Podle volby parametrů $a\,,bq\,,c$ může mít systém dva, jeden, nebo žádný rovnovážný bod. V případě dvou rovnovážných bodů je pomocí Routh–Hurwitzova kritéria ukázáno, že jeden bod je vždy nestabilní, zatímco druhý může být pro některé kombinace parametrů stabilní. Podmínky vedoucí na stabilní singulární bod jsou uvedeny teoreticky a ilustrovány numerickým experimentem. Druhou část kapitoly tvoří bifurkační analýza vzhledem k měnícímu se bifurkačnímu parametru c při fixních hodnotách $a = b = 0.1$. V této části je naznačen přechod od periodického k chaotickému chování s měnící se hodnotou c. Při přechodu lze pozorovat jev zvaný "period doubling", při kterém dochází ke zdvojnásobení period limitních cyklů. Výsledky jsou interpretovány graficky pro interval $c = [0.2, 20]$. Na tomto intervalu dojde několikrát ke zmiňovanému přechodu, který je následován kolapsem chaosu zpět na periodické chování.

Ve 4. kapitole je řešen problém stabilizace rovnovážných bodů. Jsou zde uvedeny některé přístupy a schémata možné kontroly chaotických systémů. Metoda časově zpožděného zpětnovazebního řízení Pyragasova typu, kdy řízená soustava je tvaru

$$
\mathbf{x}'(t) = f(\mathbf{x}(t)) - KI[\mathbf{x}(t) - \mathbf{x}(t - \tau)],
$$

je dále hlouběji zkoumána a aplikována pro případ dvourozměrného nestabílnho ohniska a Rösslerova systému s parametry vedoucími k chaosu. Hlavním přínosem této kapitoly je zavedení obecné podmínky pro volbu kontrolních parametrů, přesněji volbu velikosti působících rozruchů K a časového zpoždění τ. Podle uvedeného kritéria lze stanovit množinu všech (K, τ), která vede k úspěšné stabilizaci konkrétního rovnovážného bodu. Zavedené kitérium je srovnáno se známými výsledky kontroly nestabilního ohniska uvedeného v [27]. V závěru této kapitoly je prezentována množina vhodných (K, τ) pro Rösslerův systém s parametry $a = b = 0.1$ a $c = 14$. Dále jsou zde vyobrazeny konkrétní příklady různých dvojic (K, τ).

V 5. kapitole je uveden jiný přístup k otázce kontroly chaotických systémů, a to možnost synchronizace více stejných nebo různých chaotických modelů. Jsou zde teoreticky popsány vybrané přístupy a schémata různých synchronizačních metod. Kapitola je zaměřena na metody absolutní synchronizace, tj. metody, kdy dochází k úplnému splynutí trajektorií obou systémů. Konkrétní příklad synchronizace je demonstrován na dvou Rösslerových systémech se stejnými parametry pomocí schémat založených na tzv. "master-slave" vazbě a oboustranné vazbě.

V závěru je uvedeno shrnutí dosažených výsledků a jsou naznačeny možnosti dalšího výzkumu v tématu této diplomové práce, speciálně pak v oblasti synchronizace a jejího využití.

DECLARATION

I declare that I have written my master's thesis titled "Stability and chaos in nonlinear dynamical systems" independently, under the direction of my supervisor doc. RNDr. Jan Čermák, CSc. and with the use of literature and other sources of information which are all cited in the thesis and detailed in the list of literature at the end of the thesis.

Brno   . . . .
                                                                            (author's signature)

CONTENTS

INTRODUCTION

Many physical or other real-life phenomena can be described by mathematical models. A dynamical system describes evolution in time of the investigated mathematical model which is given by a system of differential or difference equations. In general, most of the models based on real problems are nonlinear and thus uneasy to solve. Particularly, there appears a numerous group of nonlinear dynamical systems across all different fields of study that evolve into chaos. Extreme sensitivity to the initial data and the impossible long-term prediction of their state is characteristical for these systems. The chaotic behaviour of certain systems had already been observed a long time ago, however, the phenomenon had not been properly investigated until the significant progress in the modern technologies in the second half of the last century.

The beginning of a great era in the chaos theory is connected to the discovery of a strange attractor by American scientist Edward Lorenz. While studying a simplified atmospheric model, Lorenz found a certain regularity in the chaotic motion. Observing the trajectory of the solution, soon it became clear, that despite the chaotic motion, the solution stays bounded inside the region of a strange attractor. Lorenz's discovery evoked a great interest in this field which was followed by many scientific works investigating other systems with similar behaviour. Over the decades, many chaotic systems have been introduced together with a complete or partial analysis of each system. Conditions for the transition from periodic behaviour to a chaotic one have also been investigated widely.

Apart from the general studies, soon there appeared a question whether the chaotic motion of a given system can be controlled or suppressed. Even though several successful methods are already known, the chaos control is still an investigated topic. Another question which arose was how two chaotic systems influence each other, more precisely, if it is possible to achieve synchrony between the motion of two chaotic systems. Again, methods providing tools for achieving certain synchrony can be easily found. Furthermore, the research in the problem of synchronization brought an interesting idea of application of chaos. The chaotic signal can be used in secure communication by hiding the information signal in randomly looking signals.

The goal of this work is to introduce the theory of chaos in dynamical systems together with several examples, present and verify some of the known results in case of Rössler system, investigate the problem of chaos control and synchronization on this model and apply the theoretical results. The thesis is organized as follows:

Chapter 1 presents an overview of basic notions and properties related to dynamical systems and chaos theory. Some of the famous dynamical systems displaying chaotic behaviour are stated in Chapter 2, e.g. the Lorenz system, the Rössler system, the Chua's systems and others.

Chapter 3 contains a deeper qualitative and numerical analysis of the Rössler dynamical system that is the simplest system (with only one nonlinear term) displaying chaos. This analysis is divided into two parts, first, the investigation of the stability of equilibrium points, and second, the characterization of the behaviour of the system with respect to a changing bifurcation parameter. The results of the analysis are verified by the results of numerical experiments.

Chapter 4 discusses methods of chaos control with a special attention paid to the time-delayed feedback control. Besides a survey of some recent results obtained by other authors, this part involves the main theoretical contribution of this thesis, namely explicit

conditions for the control gain and time delay to stabilize unstable equilibrium of a general dynamical system by use of time delayed diagonal feedback control. Also, this chapter contains series of experiments confirming and specifying the theoretical conclusions.

Finally, Chapter 5 is devoted to synchronization problem for chaotic dynamical systems. The core of this problems is specified, few basic methods are presented and illustrated via synchronization of two Rössler systems.

1 DYNAMICAL SYSTEMS AND CHAOS

The theory of chaos forms just a fraction in the theory of dynamical systems. Thus, before beginning with the discussion of chaotic models, it is important to introduce some mathematical background of dynamical systems. The following theory can be found in more details in [1], [2], [3] or [4], [5]. In general, dynamical system represents a rule describing time evolution of a state of a physical problem or a mathematical model given by a system of differential or difference equations. Under certain conditions, a current state of the system is fully determined by its previous state. If the state of the system is measured only in the integer time values, it refers to discrete dynamical systems. On the contrary, continuous measuring of time, i.e. $t \in \mathbb{R}$, refers to continuous dynamical systems. Despite the fact, that chaos can occur in both discrete and continuous dynamical systems, this work will be focused only on the continuous dynamical systems given by ordinary differential equations (ODEs). Moreover, the restriction is made to the autonomous systems of ODEs in $\mathbb{R}^n$, i.e. systems given by

$$\mathbf{x}' = f(\mathbf{x}),$$

where function $f : \mathbb{R}^n \to \mathbb{R}^n$ is a C^1 function and does not depend on the variable t. By $\mathbf{x}'$ is meant the time derivative of $\mathbf{x}$ ($\mathbf{x} = \mathbf{x}(t)$). The nonautonomous systems are not considered here, as any nonautonomous system $\mathbf{x}' = f(\mathbf{x}, t)$ with $\mathbf{x} \in \mathbb{R}^n$ can be rewritten as autonomous with $\mathbf{x} \in \mathbb{R}^{n+1}$, by letting $x_{n+1} = t$.

1.1 Definition of dynamical system

Definiton 1.1. A smooth continuous dynamical system denotes a pair $\{\Omega, \phi\}$, where Ω is a state space and $\phi : \mathbb{R} \times \Omega \to \Omega$ is a continuously differentiable function ($\phi \in C^1(\Omega)$) satisfying
   (i) $\phi_0(\mathbf{x}) = \mathbf{x}$, $\forall \mathbf{x} \in \Omega$,
   (ii) $\phi_{t+s}(\mathbf{x}) = \phi_t(\phi_s(\mathbf{x}))$, $\forall \mathbf{x} \in \Omega$ and $t, s \in \mathbb{R}$.

The function ϕ is often called an evolution operator, where $\phi_t(\mathbf{x}) = \phi(t, \mathbf{x})$.

Definiton 1.2. Let $\mathbf{x}_0 \in \Omega$ be an initial state of a system. For a fixed time $t \in \mathbb{R}$ the evolution operator ϕ transforms $\mathbf{x}_0$ into some state $\mathbf{x}(t)$ at time t, i.e.

$$\mathbf{x}(t) = \phi_t(\mathbf{x}_0).$$

Remark 1. *The state space Ω usually refers to $\mathbb{R}^n$, as it will be considered in this work.*

Definiton 1.3. Suppose an initial value problem of an autonomous system of ODEs

$$\mathbf{x}' = f(\mathbf{x}), \tag{1.1}$$
$$\mathbf{x}(t_0) = \mathbf{x}_0, \tag{1.2}$$

where $f : E \to \mathbb{R}^n$, E is an open subset of $\mathbb{R}^n$, $f \in C^1(E)$ and $\mathbf{x}_0 \in E$ is the initial value. Then $\mathbf{x}(t)$ is a solution of the initial value problem (1.1)-(1.2) on an interval I if $t_0 \in I$, $\mathbf{x}(t_0) = \mathbf{x}_0$ and $\mathbf{x}(t)$ is a solution of the system of ODEs (1.1) on the interval I.

Remark 2. *In the following chapters the function f will be assumed to be defined for all $\mathbf{x} \in \mathbb{R}^n$, i.e. $f : \mathbb{R}^n \to \mathbb{R}^n$.*

Theorem 3. *(The Existence and Uniqueness Theorem). Consider the initial value problem (1.1)-(1.2), where $f : E \to \mathbb{R}^n$, $f \in C^1(E)$. Then there exists an $a > 0$ such that the initial value problem has a unique solution $\mathbf{x}(t)$ on the interval $[-a, a]$.*

Proof. See [1] $\square$

Theorem 4. *Consider the initial value problem (1.1)-(1.2), then for each $\mathbf{x}_0 \in E$ there is a maximal interval $J = (\alpha, \beta)$ on which the initial value problem has a unique solution $\mathbf{x}(t)$.*

Proof. See [1] $\square$

Definiton 1.4. Let $E \subseteq \mathbb{R}^n$ and $f \in C^1(E)$. Let $\phi(t, \mathbf{x}_0)$ be the solution of (1.1)-(1.2) defined on its maximal interval $J(\mathbf{x}_0)$, $\mathbf{x}_0 \in E$. Then for $t \in J(\mathbf{x}_0)$, the family of evolution operators ϕ_t defined by

$$\phi_t(\mathbf{x}_0) = \phi(t, \mathbf{x}_0) \tag{1.3}$$

is called the flow of the system (1.1). ϕ_t is often referred to as the flow of the vector field f.

Definiton 1.5. Suppose the initial value $\mathbf{x}_0$ is fixed and $J = J(\mathbf{x}_0)$. Then the mapping $\phi(\cdot, \mathbf{x}_0) : J \to E$ defines a solution curve or a trajectory of the system (1.1) through the point $\mathbf{x}_0 \in E$. The trajectory is visualized as a motion along a curve Γ through the point $\mathbf{x}_0$. The arrow then indicates the orientation of the curve as time increases.

The phase portrait of the system (1.1) refers to the set of all solution curves of (1.1) for different initial points satisfying the initial value problem (1.1)-(1.2) in the phase space. The solution curves in the phase space never intersect each other.

Definiton 1.6. A point $\mathbf{x}^* \in E$ is called equilibrium point (fixed point, critical point) of the system (1.1) if $f(\mathbf{x}^*) = \mathbf{0}$ ($\mathbf{0}$ means the zero vector). Moreover, for any trajectory starting in $\mathbf{x}^*$, i.e. $\mathbf{x}(0) = \mathbf{x}^*$, is $\mathbf{x}(t) = \phi_t(\mathbf{x}^*) \equiv \mathbf{x}^*$ for any $t \in \mathbb{R}$.

In general, trajectories of the solution $\mathbf{x}(t)$ can be divided into 3 main categories:
  (i) Fixed point - the solution $\mathbf{x}(t)$ is constant, i.e. trajectory stays in the fixed point for all time.
 (ii) Cycle, periodic orbit - the solution $\mathbf{x}(t)$ is periodic, i.e. the trajectory forms a closed curve and stays on this curve for all time.
(iii) Open curve - the trajectory is an injective map never intersecting itself.

1.2 Linear dynamical system

Suppose the system given in (1.1) is linear, i.e. function f consists of linear terms only, $f : \mathbb{R}^n \to \mathbb{R}^n$. Then the system can be rewritten as

$$\mathbf{x}' = A\mathbf{x},$$

where $\mathbf{x} \in \mathbb{R}^n$, A is an $n \times n$ matrix and the following theorem holds.

Theorem 5. *(The Fundamental Theorem for Linear Systems). Let A be an $n \times n$ matrix. Then for a given $\mathbf{x}_0 \in \mathbb{R}^n$, the initial value problem $\mathbf{x}' = A\mathbf{x}$, $\mathbf{x}(0) = \mathbf{x}_0$ has a unique solution for all $t \in \mathbb{R}$ given by*

$$\mathbf{x}(t) = e^{At}\mathbf{x}_0.$$

Proof. See [1] □

1.3 Nonlinear dynamical system

According to Theorem 3, a unique solution of an initial value problem of a nonlinear system exists on some interval I. However, unlike the linear cases, very few nonlinear systems can be solved analytically. The investigation of behaviour of nonlinear systems usually consists of analytical, geometrical, and topological techniques. Numerical methods play also very important role in such analysis.

Linearization of nonlinear systems

Nonlinear systems are often investigated in the neighborhood of its equilibrium points. It can be shown that the local behaviour of the nonlinear system $\mathbf{x}' = f(\mathbf{x})$ near a hyperbolic equilibrium point $\mathbf{x}^*$ is qualitatively determined by the behaviour of the linear system $\mathbf{x}' = A(\mathbf{x})$, where A is the Jacobian matrix evaluated at point $\mathbf{x}^*$.

Remark 6. *Recall, the Jacobian matrix J evaluated at a fixed point $\mathbf{x}^* \in \mathbb{R}^n$ is given by $n \times n$ matrix*

$$J = Df(\mathbf{x}^*) = \begin{pmatrix} \frac{f_1(\mathbf{x}^*)}{\partial x_1} & \cdots & \frac{f_1(\mathbf{x}^*)}{\partial x_n} \\ \vdots & \ddots & \vdots \\ \frac{f_n(\mathbf{x}^*)}{\partial x_1} & \cdots & \frac{f_n(\mathbf{x}^*)}{\partial x_n} \end{pmatrix}.$$

The eigenvalues λ of the Jacobian matrix can be computed as the roots of characteristic polynomial

$$P(\lambda) = det\,(J - \lambda I),$$

where I represents the identity matrix.

Definiton 1.7. An equilibrium point $\mathbf{x}^*$ of the system (1.1) is called hyperbolic if none of the eigenvalues of the Jacobian matrix $J = Df(\mathbf{x}^*)$ has zero real part. Otherwise, the equilibrium point is called nonhyperbolic.

If the fixed point $\mathbf{x}^*$ is hyperbolic, then according to Hartman-Grobman Theorem [1] there exists a neighborhood of this point, in which the nonlinear system $\mathbf{x}' = f(\mathbf{x})$ is topologically conjugate to the system $\mathbf{x}' = A(\mathbf{x})$, where A is the linearization matrix, i.e. $A = Df(\mathbf{x}^*)$.

1.4   Stability

Generally, stability of a solution is determined by the sensitivity to a perturbation of the initial data. The solution is called stable if a small perturbation of initial data yields a small change in the solution. Furthermore, the solution is called attractive or asymptotically stable if the deviation of the solution caused by a perturbation of initial data will disappear as $t \to \infty$. In dynamical systems, it is more common to refer to a stability of equilibrium points of the given system.

Definiton 1.8. Let ϕ_t denotes the flow of the system (1.1) defined for all $t \in \mathbb{R}$. An equilibrium point $\mathbf{x}^*$ is (locally) stable if for all $\varepsilon > 0$ there exists a $\delta > 0$ such that for all $\mathbf{x} \in N_\delta(\mathbf{x}^*)$ and $t \geq 0$ then

$$\phi_t(\mathbf{x}) \in N_\varepsilon(\mathbf{x}^*).$$

Furthermore, $\mathbf{x}^*$ is (locally) asymptotically stable if it is stable and if there exists a $\delta > 0$ such that for all $\mathbf{x} \in N_\delta(\mathbf{x}^*)$,

$$\lim_{t \to \infty} \phi_t(\mathbf{x}) = \mathbf{x}^*.$$

The equilibrium point is said to be unstable if it is not stable.

Remark 7. *Similarly, these stability notions are used for other significant solutions of the system (1.1) (e.g. periodic solutions).*

The basic tool for stability analysis of equilibrium points is provided by the linearization method. The stability of a fixed point can be determined by the sign of real parts of eigenvalues λ of the Jacobian matrix. The following theorem holds.

Theorem 8. *Let $J = Df(\mathbf{x}^*)$ be the Jacobian matrix for the system (1.1) evaluated at a fixed point $\mathbf{x}^*$ and let λ_i be its eigenvalues.*
  (i) *If $\Re(\lambda_i) < 0$ for all λ_i, then the fixed point $\mathbf{x}^*$ is asymptotically stable.*
  (ii) *If $\Re(\lambda_i) > 0$ for at least one λ_i, then the fixed point $\mathbf{x}^*$ is unstable.*
  (iii) *If $\Re(\lambda_i) = 0$ for at least one λ_i, then the fixed point $\mathbf{x}^*$ is nonhyperbolic and its stability cannot be determined by the linearization method.*

Classification of basic fixed points can be found in the literature. [1] For further investigation of nonhyperbolic points, it is possible to use other methods which can help to determine their stability. The stability according to Lyapunov is defined as follows.

Theorem 9 (Lyapunov Function). *Suppose the nonlinear system (1.1) with an equilibrium point $\mathbf{x}^*$, $\mathbf{x}^* \in E$, where E is an open subset in $\mathbb{R}^n$. Now, suppose that there exists a function $V : E \to \mathbb{R}^n$ satisfying*
  (i) *$V(\mathbf{x}^*) = 0$,*
  (ii) *$V(\mathbf{x}) > 0$ if $\mathbf{x} \neq \mathbf{x}^*$.*
Then
  (i) *if $\dot{V}(\mathbf{x}) \leq 0$ for $\forall \mathbf{x} \in E$, $\mathbf{x}^*$ is stable,*
  (ii) *if $\dot{V}(\mathbf{x}) < 0$ for $\forall \mathbf{x} \in E \setminus \{\mathbf{x}^*\}$, $\mathbf{x}^*$ is asymptotically stable,*
  (iii) *if $\dot{V}(\mathbf{x}) > 0$ for $\forall \mathbf{x} \in E \setminus \{\mathbf{x}^*\}$, $\mathbf{x}^*$ is unstable.*
The function V is called the Lyapunov function. The term $\dot{V}(\mathbf{x}) = DV(\mathbf{x})f(\mathbf{x})$, where $DV = (\frac{\partial V}{\partial x_1}, \dots, \frac{\partial V}{\partial x_n})$.

Proof. See [1]   □

1.5   Routh–Hurwitz Criterion

If the dynamical system has a dimension grater than two, it is often almost impossible to express the eigenvalues of characteristic polynomial. Therefore, the following criterion gives an algebraic tool for verification if the characteristic equation has roots in the left half of the complex plane. [6]

Theorem 10 (Routh–Hurwitz Criterion). *Given the polynomial,*

$$P(\lambda) = \lambda^n + a_1\lambda^{n-1} + \ldots + a_{n-1}\lambda + a_n,$$

where a_i are real constants, $i = 1, \ldots, n$, define the n Hurwitz matrices using the coefficients a_i of $P(\lambda)$:

$$H_1 = (a_1), \quad H_2 = \begin{pmatrix} a_1 & 1 \\ a_3 & a_2 \end{pmatrix}, \quad H_3 = \begin{pmatrix} a_1 & 1 & 0 \\ a_3 & a_2 & a_1 \\ a_5 & a_4 & a_3 \end{pmatrix},$$

and

$$H_n = \begin{pmatrix} a_1 & 1 & 0 & 0 & l\ldots & 0 \\ a_3 & a_2 & a_1 & 1 & \ldots & 0 \\ a_5 & a_4 & a_3 & a_2 & \ldots & 0 \\ \vdots & \vdots & \vdots & \vdots & \ldots & \vdots \\ 0 & 0 & 0 & 0 & \ldots & a_n \end{pmatrix}, \; for \; n > 3.$$

Coefficients $a_j = 0$ if $j > n$. All of the roots of the polynomial $P(\lambda)$ are negative or have negative real part if and only if the determinants of all Hurwitz matrices are positive, i.e.

$$\det H_j > 0, \quad j = 1, 2, \ldots, n.$$

Then, particularly for $n = 3$ the criteria can be given as

$$a_1 > 0 \,, a_3 > 0 \,, \; and \; a_1 a_2 > a_3.$$

1.6   Bifurcation

Bifurcation theory studies the qualitative behaviour of the system (1.1) as the vector field f changes. If the qualitative behaviour of the system remains unchanged for all nearby vector fields, then the system (or the vector field f) is said to be structurally stable. On the contrary, if the vector field is not structurally stable, it belongs to the bifurcation set.

In other words, bifurcation can be explained as follows. Suppose that the system depends on a parameter $\mu \in \mathbb{R}$ (or a set of parameters $\mu \in \mathbb{R}^m$). Then the system is given by

$$\mathbf{x}' = f(\mathbf{x}, \mu).$$

A bifurcation occurs in the system when a small smooth change made to the bifurcation parameter μ causes a sudden change in the qualitative behaviour. The value of the parameter at this change is known as the bifurcation value or a critical value of bifurcation parameter μ.

The structural changes of the system usually refer to the changes in stability of significant solutions (e.g. equilibrium points, periodic orbits) or to the appearance of new significant solution as parameter passes the critical value.

1.7 Attractors

Attractor can be defined as a closed set A in the phase space with the following properties:

  (i) A is an invariant set, i.e. any trajectory starting in A stays in A for all the time.

 (ii) A attracts an open set of initial conditions, i.e. there is an open set $U, A \subseteq U$ such that if $\mathbf{x} \in U$, $\phi_t(\mathbf{x}) \in U$ for all $t \geq 0$ and $\phi_t(\mathbf{x}) \to A$ as $t \to \infty$.

(iii) A is minimal, i.e. there is no proper subset of A that satisfies the previous conditions.

In other words, an attractor is a specific set that attracts all trajectories in its neighborhood. There are three types of so-called nonstrange attractors, namely fixed point attractor, limit cycle attractor and torus attractor. A particular attractor, which was observed in chaotic systems is called a strange attractor and its definition leads to fractal theory, i.e. theory of sets with non-integer dimension. [7]

1.8 Chaos

By the term chaos, it is understood a randomly looking, aperiodic long-term behaviour of a deterministic dynamical system, which exhibits sensitive dependence on initial conditions. This means, that two trajectories starting in the infinitesimal neighbourhood can reach completely different positions after some time. In continuous dynamical systems, chaos can occur only in 3 and higher-dimensional spaces.

Chaotic behaviour of a system can be revealed by computation of the Lyapunov exponents. If at least one of the exponents from the Lyapunov spectrum is positive then the system is chaotic in nature.

Lyanupov exponents

Lyapunov exponents measure the sensitivity of a dynamical system to small changes in initial conditions. Therefore, it is a useful tool for identifying chaos in dynamical systems.

The Lyapunov exponent can be defined by the following. Let d_0 be the distance of two close points at t_0. After time t the separation of the trajectories starting at these points is given by

$$d \sim d_0 e^{\Lambda(t-t_0)}.$$

The Λ is called the Lyapunov exponent. This definition, however, provides the value for two specific neighbouring points over a specific interval of time. Thus, to approximate the exponent for entire system, it is necessary to take an average of many different neighbourhoods.

Definiton 1.9. If the displacement between the i-th point and a neighbouring point at time t_i is d_i, and the initial displacement between these two points is d_{0i} at time t_{0i}, then the Lyapunov exponent is defined as

$$\Lambda = \lim_{n \to \infty} \frac{1}{n} \sum_{i=1}^{n} \frac{1}{(t_i - t_{0i})} \ln |d_i/d_{0i}|.$$

Moreover, a system defined in n-dimensions has n exponents, one for each dimension. The set of all exponents is called the Lyapunov spectrum. If one of the exponents is positive then chaos occurs in the system. [8], [9].

2 EXAMPLES OF CHAOTIC SYSTEMS

The theory of chaos has achieved a great interest since the Lorenz's discovery. Nowadays, a good deal of chaotic systems can be found across all different fields of science. In this chapter, some of the most famous models will be introduced, including short explanation, graphical demonstration and potential use. General information about some of the systems introduced in this chapter can be found in [7], [10], [11], [12].

The common property of chaotic systems is the strong dependence on the choice of system parameters and initial values. Considering the first observation, it is important to remember that many combinations of system parameters do not necessarily lead to chaotic behaviour at all. Some of the specific choices for which the chaos occurs will be given along with each presented model. For deeper investigation of suitable choices, it is necessary to run an analysis of the system, comparing the influence of the parameters in the equilibrium points. Later in this work, analysis of suitable values of the Rössler system will be discussed.

The graphical demonstration will be given using MATLAB's function ode45. This function is a standard MATLAB's solver for ordinary differential equations based on an algorithm of Dormand and Prince, which is an explicit Runge–Kutta 4th/5th order method. It is a single-time step method containing the correction of the step size according to error estimation. For this work, the maximum step-size was improved to achieve smoother solutions.

2.1 Lorenz's system

Lorenz's system is probably the best known deterministic nonlinear system exhibiting chaotic behaviour. The model was named after an American mathematician and meteorologist Edward Norton Lorenz who was studying a simplified model of convection rolls in the atmosphere, trying to explain some unpredictable weather evolutions. Some may recognise the system as The Butterfly Effect.

Behind the poetic name, The Butterfly Effect, are two hidden meanings. First one gives a popular metaphorical simplification of a chaos development, saying that even a single flap of butterfly's wings can cause a storm far away from its location. In reality, it means that the system is so dependent on the initial values that even a small change in one state can cause great differences in some later state. In meteorology, this explains why the forecast in the longer term is very unreliable since even a slight disturbance from the known weather evolution may result in very different behaviour after some time. The second meaning is connected to the 3D phase portrait of the systems (Figure 2.1), which is reminiscent of the shape of butterfly's wings.

Lorenz's goal was to find a system of differential equations that would correspond to and simplify the real problem. His approach can be explained in brief as follows: imagine the atmosphere as a single fluid particle which is heated from below and cooled from above. Thanks to the heating the particle rises up but the cooling makes it fall back down again, and the process can repeat. In general, the model of the atmosphere is very complex since changes in temperature, pressure, wind velocity, etc., must be considered.

Lorenz simplified the problem with the help of the techniques as Oberbeck-Boussinesq approximation, Rayleigh-Bénard convection (describing the fluid circulation between two

horizontal layers of different temperature), Galerkin method, and finally the key equations of fluid dynamics, such as the continuity equation, Navier–Stokes equations and Fourier law. [3] The final Lorenz's model, consists of 3 nonlinear ordinary differential equations in $\mathbb{R}^3$ containing three positive parameters and two nonlinear (quadratic) terms. The equations determining the Lorenz's model are

$$
\begin{aligned}
x' &= \sigma(y - x)\,, \\
y' &= rx - y - xz\,, \\
z' &= xy - bz\,,
\end{aligned}
$$

where σ, r, $b > 0$ are system parameters. Parameter σ stands for the Prandtl number, r for the Rayleigh number and b is a parameter related to the physical size of the system. The nonlinearity is present in the second and third equations in the terms xz and xy.

The most famous phase portrait of Lorenz's system corresponds to the choice of parameters $\sigma = 10$, $r = 28$, $b = 8/3$. From Figure 2.1, it is easy to understand the first reason why the name 'Butterfly effect' is used.
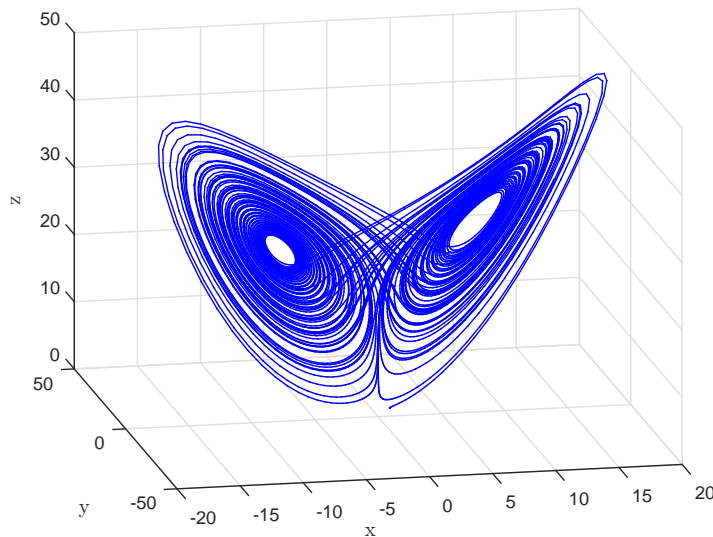
Figure 2.1: The Lorenz's model ($\sigma = 10$, $r = 28$, $b = 8/3$).

While studying the system, Lorenz came to a great discovery, and he showed that despite the chaos, there exists a complicated structure which gives certain limitation to the developement of the trajectories. In other words, despite the fact that the solution of the model for certain parameters behaves irregularly and never repeats itself exactly, it remains in some bounded region of the phase space. This structure was later named a strange attractor and leads to the theory of fractals. Above that, another important property of the system is its symmetry. If $(x(t),\ y(t),\ z(t))$ is a solution, so is $(-x(t),\ -y(t),\ z(t))$. Further details about the system can be found in [3], [10].

In practice, the Lorenz's system does not give the weather forecast. However, its properties are very useful when applied to collected statistical data. Besides atmospheric convection, there are several other applications of Lorenz's system. For example, the same equations appear in models for lasers, electric circuits or dynamos. Moreover, the

equations can describe motion of a specially designed waterwheel with leaky cups regularly placed on the wheel. The cups on the wheel are getting filled with water, and the wheel is turning to the side where the gravitational force is greater. For a certain flow, velocity and amount of water in each cup it suddenly becomes impossible to determine which way will the wheel turn. [7]

The fact, that the chaotic systems are highly sensitive to the choice of initial conditions is demonstrated in Figure 2.2. Two initial conditions were taken from a small neighborhood, precisely $\mathbf{x}_0^1$ and $\mathbf{x}_0^2$ differ only in the y-variable by value 0.1. Yet, the trajectories separate fast from each other in time.
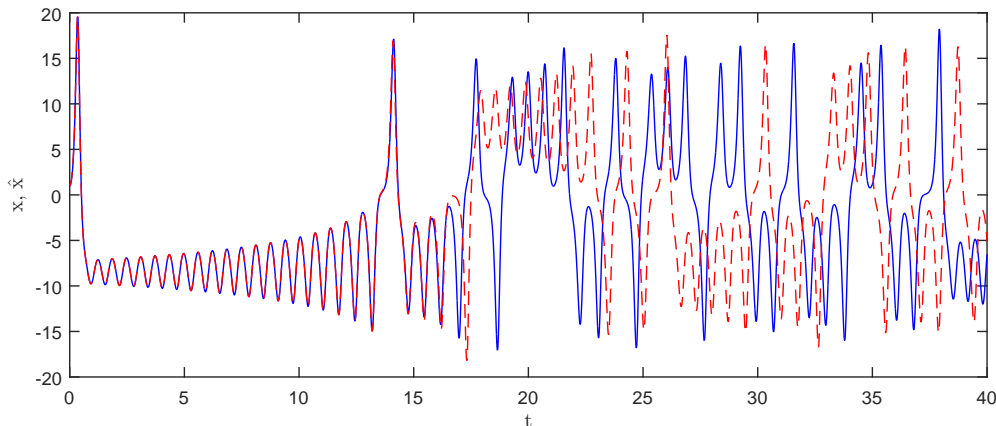
Figure 2.2: Lorenz's model; evolution of variable x for 2 initial points.

2.2 Rössler system

Another well-known model with chaotic behaviour is the Rössler system, which was studied by a German biochemist Otto Rössler. After the discovery of the Lorenz attractor, lots of studies appeared, trying to find similar results in different fields. Rössler set a different goal for himself, to find a model which behaves similarly to the Lorenz's one but is easier to solve. He presented a theoretical model fulfilling his aims. The system of Rössler evolves into chaos and compared to the previous model there appears only one nonlinear term in the equations. Moreover, the system was later found to be useful in modelling equilibrium states in chemical reactions. The Rössler system is also considered to be a minimal system for continuous chaos. That is achieved for at least three reasons: its phase space has the minimal dimension possible for chaos appearance, its nonlinearity is made by a single quadratic term, and it generates a chaotic attractor with a single lobe.

Rössler discovered more chaotic systems, including the first 4D hyperchaotic attractor. However, the following model with three real parameters a, b, c, became the most famous.

$$
\begin{aligned}
x' &= -y - z\,, \\
y' &= x + ay\,, \\
z' &= b + z(x - c)\,.
\end{aligned}
$$

In his work, Rössler investigated the chaotic behaviour for the combination of parameters $a = 0.2$, $b = 0.2$ and $c = 5.7$ as can be seen in Figure 2.3. [13]
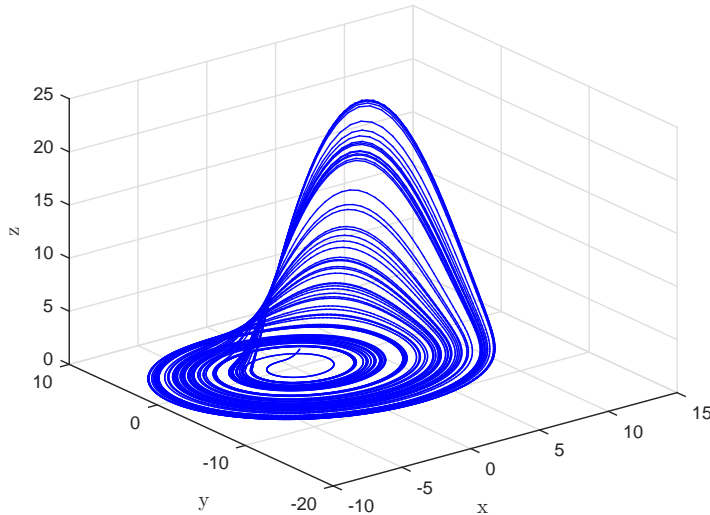
Figure 2.3: Rössler system ($a = 0.2$, $b = 0.2$ and $c = 5.7$).

Later, another combination $a = 0.1$, $b = 0.1$ and $c = 14$ started to appear more often in the studies. In both cases, a simple attractor can be observed. However, for another combination a different type of attractor appears. For example, for a choice $a = 0.343$, $b = 1.82$ and $c = 9.75$ a screw-type attractor appears. This can be seen in Figure 2.4.
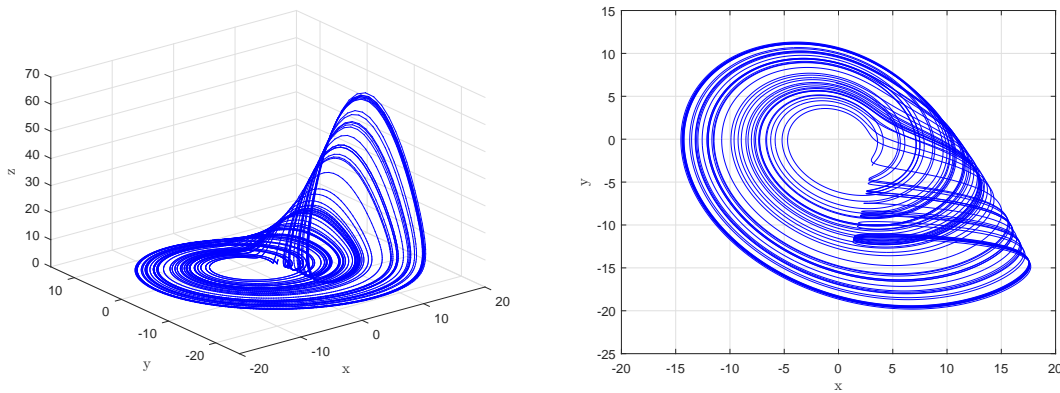

Figure 2.4: Rössler system ($a = 0.343$, $b = 1.82$ and $c = 9.75$).

The Rössler model will be further discussed within this work. More details will be therefore given in the following chapters.

2.3   Chua's circuit

The nonlinear electronic circuits form another field of study where chaos occurs widely. The most famous and theoretically well described one is Chua's circuit. This simply constructed circuit was invented by an American electrical engineer and computer scientist Leon Ong Chua in 1983. The third-order RLC circuit contains four linear elements (two

capacitors, inductor and linear resistor) and one nonlinear element (nonlinear resistor R_n, sometimes called 'Chua's diode'). The scheme of the circuit is shown in Figure 2.5.
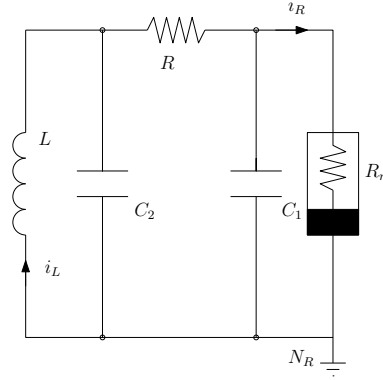

Figure 2.5: Chua's circuit. [11]

Using the Kirchhoff's circuit laws the circuit is described by equations

$$C_1 \frac{dv_{C_1}}{dt} = G(v_{C_2} - v_{C_1}) - f(v_{C_1}),$$

$$C_2 \frac{dv_{C_2}}{dt} = G(v_{C_1} - v_{C_2}) + i_L,$$

$$L \frac{di_L}{dt} = v_{C_2},$$

with usual indication: i stands for current, $G = 1/R$ is the conductance of a resistor and indexes $C_{1,2}$ stand for capacitors, L for inductor. The nonlinear element is given by function $f(v_{C_1}) = m_0 v_{C_1} + \frac{1}{2}(m_1 - m_0)[|v_{C_1} + B_p| - |v_{C_1} - B_p|]$ describing the electrical response of the nonlinear resistor.

For mathematical analysis, it is more common to use a dimensionless model which is referring to Chua's circuit given by

$$x' = \alpha[y - x - f(x)],$$
$$y' = x - y + z,$$
$$z' = -\beta y,$$

where $x = v_{C_1}/B_p$, $y = v_{C_2}/B_p$, $z = i/B_p G$, $\alpha = C_2/C_1$, $\beta = C_2/G^2 L$ and finally $f(x) = bx + \frac{1}{2}(a - b)[|x + 1| - |x - 1|]$ with $a = m_1/G$, $b = m_0/G$. [11]

The system is also interesting for the tendency to produce different kinds of attractors for different combinations of system parameters which are shown in Figures 2.6 and 2.7. In the following figures, a simple attractor and a double-scroll attractor can be seen. Moreover, the system is invariant under the transformation $(x, y, z) \rightarrow (-x, -y, -z)$. The Chua's circuit is often used as a physical source of pseudo random signals. Further, the system is implemented in the experiments on secure communication by chaotic systems.
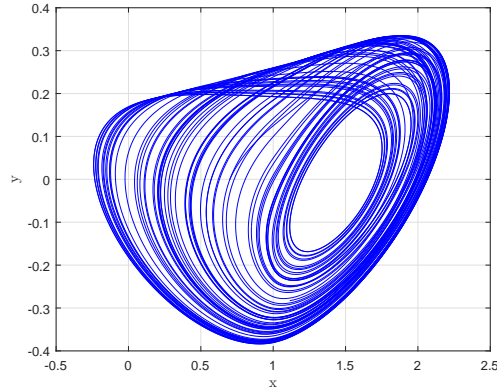
The case of simple attractor:

Figure 2.6: Chua's circuit ($\alpha = 9.4$, $\beta = 16$, $m_0 = -8/7$ and $m_1 = -5/7$).
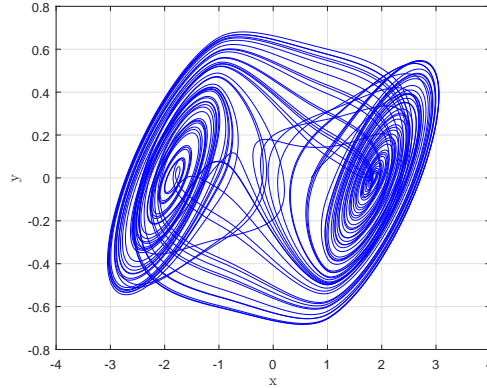
The case of double-scroll attractor:

Figure 2.7: Chua's circuit ($\alpha = 10$, $\beta = 14.87$, $m_0 = -1.27$ and $m_1 = -0.68$).
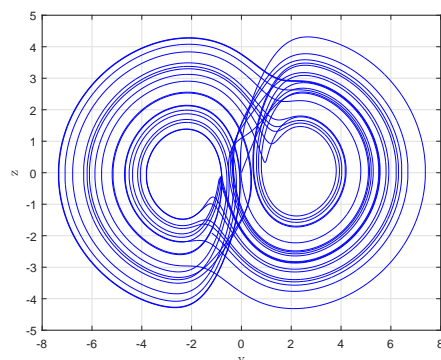
2.4 Modified Van der Pol's Oscillator

One of the lesser known but very interesting system is the modified model of Van der Pol's oscillator. The original Van der Pol's oscillator analysis the dynamic behaviour of (self) excited oscillations. The system is of dimension 2 and the solution is periodic. By modifying the system with a feedback loop, it is possible to achieve chaotic behaviour. According to [14], equations of Van der Pol's oscillator can be modified and applied in economics. It is possible to find a heuristic model of economic cycles focused on the capital flight observed in the less developed countries. The new system in 3D is of the form

$$
\begin{aligned}
x' &= ky + \mu x(b - y^2)\,, \\
y' &= -x + sz\,, \\
z' &= px - qy\,,
\end{aligned}
$$

where k, μ, b, s, p and q are positive parameters. In economics, the variables x, y, and z represent dimensionless variables of savings, gross domestic product, and foreign capital inflow. The main parameter of interest is s, since it corresponds to the feedback loop. Therefore, by varying s the system can be changed from periodic to chaotic and vice-versa. For some interval of s the system is also antisymmetric. To demonstrate that the structure of chaos is changing with varying s the following parameters were chosen and depicted in Figure 2.8; $k = 0.02$, $\mu = 0.4$, $b = 0.2$, $p = 10$, $q = 0.1$, s was taken to be $s_1 = 0.2$, $s_2 = 35$ and $s_3 = 150$.
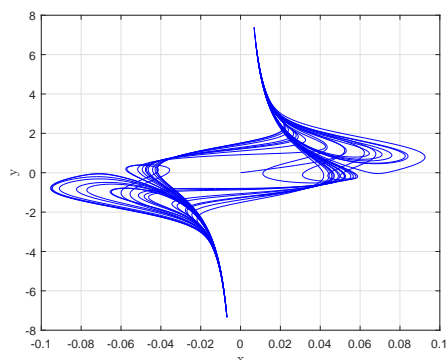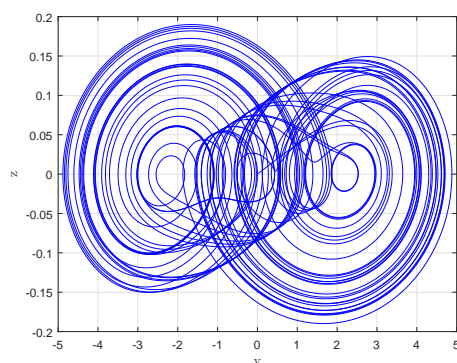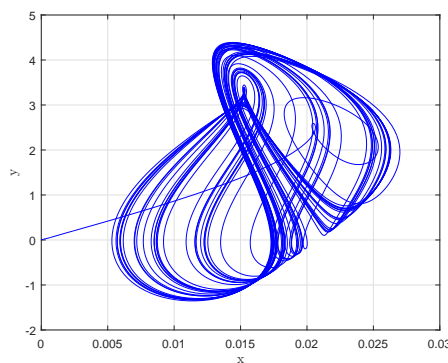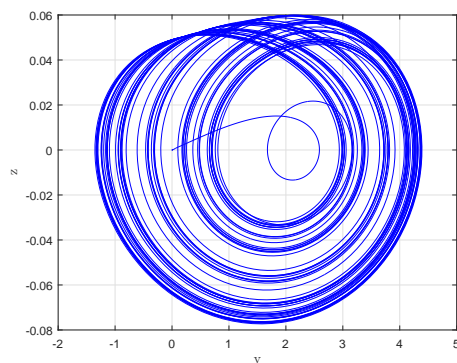

(a) $s_1 = 0.2$; xy-plane.

(b) $s_1 = 0.2$; yz-plane.
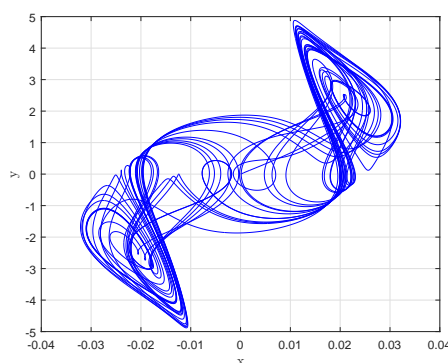
(c) $s_2 = 35$; xy-plane.

(d) $s_2 = 35$; yz-plane.

(e) $s_3 = 150$; xy-plane.

(f) $s_3 = 150$; yz-plane.

Figure 2.8: Modified Van der Pol's Oscillator; different values of s.

2.5   Belousov–Zhabotinsky reaction

As well as the chaotic systems in physics, one can find strange behaviour also in chemistry. In 1951, Boris Belousov discovered a chemical reaction which oscillated between the state when the solution is colourless and when it is yellow due to ions of its catalyst. However, Belousov's discovery was not accepted at first, and it took some years before the problem was introduced in papers. In the late '70s, his work was further investigated and discussions over whether the reaction exhibits only limit-cycle oscillations or if there are some conditions for which chaos can occur were made. Several approaches were used in order to find the answer to this question.

The most famous are probably The Oregonator and The Györgyi-Field Model. The Oregonator gave a great simplification reducing the model into 3 differential equations. Unfortunately, this model did not succeed to allow the observation of chaos. On the contrary, the second model introduced by Györgyi and Field was more successful. By allowing the reaction to happen in continuous-flow stirred tank reactor, they proved the theory that chaos can occur in chemical systems when the reaction starts far from the equilibrium. During the next years, many more studies appeared replacing the cerium catalyst to ferroin catalyst or others, reaching very similar results. [15]

The derivation of this system is out of the scope of this chapter since many chemical species appear during the reaction. However, more information can be found in [7], [16] and [17]. The following system of equations describes The Györgyi-Field Model and can be found in more details in [17] together with the appropriate parameters and phase portrait.

$$
\frac{dx}{d\tau} = T_0[-k_1 H Y_0 x\bar{y} + k_2 A H^2 Y_0 X_0^{-1}\bar{y} - 2k_3 X_0 x^2 +
$$
$$
+ \frac{1}{2}k_4 A^{1/2} H^{3/2} X_0^{-1/2}(C - Z_0 z)x^{1/2} - \frac{1}{2}k_5 Z_0 xz - k_f x]
$$
$$
\frac{dz}{d\tau} = T_0[k_4 A^{1/2} H^{3/2} X_0^{1/2}(C/Z_0 - z)x^{1/2} - k_5 X_0 xz -
$$
$$
- \alpha k_6 V_0 zv - \beta k_7 Mz - k_f z]
$$
$$
\frac{dv}{d\tau} = T_0[2k_1 H X_0 Y_0 V_0^{-1} x\bar{y} + k_2 A H^2 Y_0 V_0^{-1}\bar{y} + k_3 X_0^2 V_0^{-1} x^2 -
$$
$$
- \alpha k_6 Z_0 zv - k_f v],
$$

where $\tau = t/T_0$, $x = X/X_0$, $z = Z/Z_0$, $v = V/V_0$
$$
\bar{y} = [\alpha k_6 Z_0 V_0 zv/(k_1 H X_0 x + k_2 A H^2 + k_f)]/Y_0.
$$

In the equations x, z, v represent dimensionless variables of the chemical components $Y = Br^-$, $X = HBrO_2$, $Z = Ce^{4+}$, $V = BrCH(COOH)_2$, $A = BrO_3^-$, $H = H^+$, and $M = CH_2(COOH)_2$. Out of the other parameters the most important one is k_f since in varying k_f the system's behaviour can change to chaotic.

2.6 Other chaotic models

One can see now, that chaos became a widely investigated topic. Many systems were discovered or built across all the fields of study, especially in electrics, biology, physics or economics. In the rest of this chapter some more examples of chaotic systems will be given in brief.

2.6.1 Double pendulum

Double pendulum, as the name suggests, is a pendulum with another one attached to its end point (see Figure 2.9). The motion of the pendulum is described by a system of nonlinear ODEs. The system solution depends on the length of the two limbs holding the pendulums. The trajectory of any double pendulum system is strongly influenced by initial conditions involving initial position and velocity. [18]
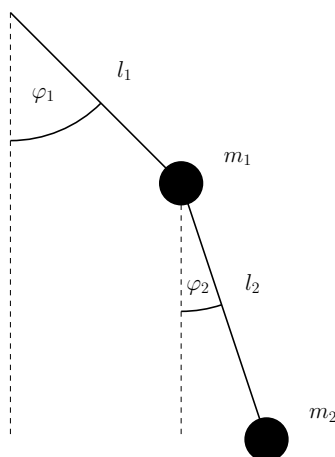

Figure 2.9: Double pendulum. [18]

2.6.2 Sprott systems

There exist even simpler examples of chaotic systems than the ones presented by E. Lorenz or O. Rössler. J. C. Sprott presented a group of 18 different models of chaos that contain either six terms and one quadratic nonlinearity or five terms and two quadratic nonlinearities. An overview of this group can be found in his book [12]. The models can be easily applied to electric circuits.
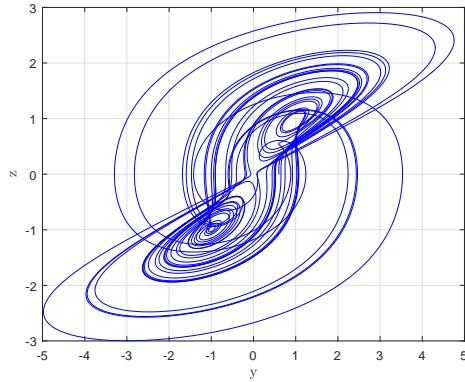
The model SQB depicted in Figure 2.10a is given by a system of equations

$$x' = yz \,,$$
$$y' = x - y \,,$$
$$z' = 1 - xy \,.$$

Another example presented by Sprott is system SQL

$$x' = y + 3.9z \,,$$
$$y' = 0.9x^2 - y \,,$$
$$z' = 1 - x \,,$$

which is depicted in Figure 2.10b.
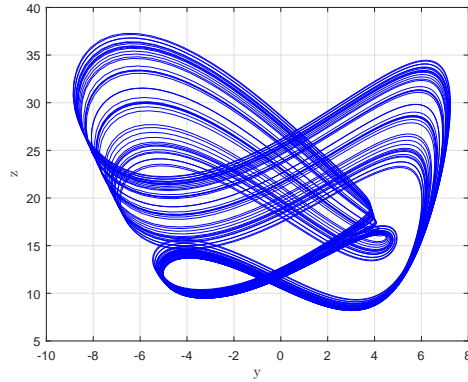
(a) System SQB.   (b) System SQL.

Figure 2.10: Sprott systems SQB and SQL.

2.6.3   Chen system

Besides the Chua's system, another example of a double-scroll attractor is the Chen system. This system was discovered by anticontrol method (sometimes called chaotification) and it is similar to Lorenz's system as they differ from each other in only one equation. [19] On the other hand, there are certain differences both in the phase portraits and suitable parameters leading to chaos. The Chen system is given by

$$
\begin{aligned}
x' &= a(y - x)\,, \\
y' &= (c - a)x - xz + cy\,, \\
z' &= xy - bz\,,
\end{aligned}
$$

where a, b, c are positive real parameter. The characteristic trajectory for parameters $a = 35, b = 3, c = 28$ is given in Figure 2.11.
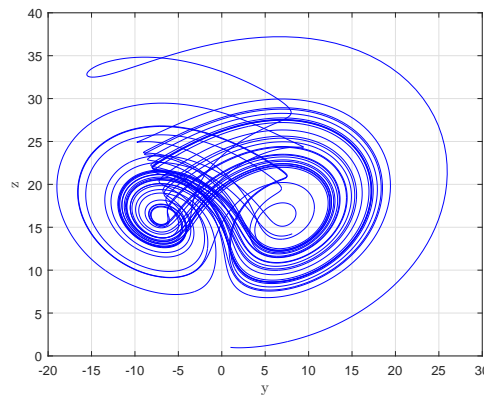

Figure 2.11: Chen system $(a = 35, b = 3, c = 28)$.

3 ANALYSIS OF RÖSSLER SYSTEM

Up to this point, a list of chaotic models was presented in brief as well as a basic theory for nonlinear dynamical systems. In the sequel, the attention will be paid to the stability analysis of the Rössler system. Namely, the local behaviour will be investigated in the neighbourhood of its equilibrium points. In order to show the changes in the evolution of the system, some more phase portraits will be included as a result of numerical analysis for various parameters. In the end, specific cases of bifurcation analysis will be presented for the fixed choice of parameters $a = b = 0.1$ and c varying. Recall, that the system is given by equations

$$
\begin{aligned}
x' &= -y - z\,, \\
y' &= x + ay\,, \\
z' &= b + z(x - c)\,,
\end{aligned}
\tag{3.1}
$$

where a, b, c are real parameters. For the later work, all parameters will be assumed to be positive.

3.1 Equilibrium points

As was defined earlier, an equilibrium point of a system

$$
\mathbf{x}' = f(\mathbf{x})
$$

is every point $\mathbf{x}^*$ for which $f(\mathbf{x}^*) = 0$. Hence, fixed points of the Rössler system (3.1) are given as a solution of

$$
\begin{aligned}
0 &= -y - z\,, \\
0 &= x + ay\,, \\
0 &= b + z(x - c)\,.
\end{aligned}
$$

Taking $y = -z$, $x = az$, and substituting them into the third equation, z can be expressed as the roots of quadratic equation $az^2 - cz + b = 0$. Thus

$$
z_{1,2} = \frac{c \pm \sqrt{c^2 - 4ab}}{2a}\,.
$$

Now three cases are possible: If the condition $c^2 > 4ab$ is fulfilled, then there exist two equilibrium points

$$
\mathbf{x}_1^* = \left[\frac{c}{2} + \frac{\sqrt{c^2 - 4ab}}{2}, -\frac{c}{2a} - \frac{\sqrt{c^2 - 4ab}}{2a}, \frac{c}{2a} + \frac{\sqrt{c^2 - 4ab}}{2a} \right]\,,
\tag{3.2}
$$

$$
\mathbf{x}_2^* = \left[\frac{c}{2} - \frac{\sqrt{c^2 - 4ab}}{2}, -\frac{c}{2a} + \frac{\sqrt{c^2 - 4ab}}{2a}, \frac{c}{2a} - \frac{\sqrt{c^2 - 4ab}}{2a} \right]\,,
\tag{3.3}
$$

while for $c^2 = 4ab$ there is only one equilibrium point

$$
\mathbf{x}^* = \left[\frac{c}{2}, -\frac{c}{2a}, \frac{c}{2a} \right]\,.
\tag{3.4}
$$

In the last case, $c^2 < 4ab$, no equilibrium point exists.

3.2 Stability of equilibrium points

To determine the nature of an equilibrium point and the behaviour in its neighbourhood, the linearization method can be used. Firstly, the Jacobian matrix needs to be built by computing partial derivatives of all components of (3.1). The Jacobian matrix for the Rössler system evaluated at an equilibrium point $\mathbf{x}^* = [x^*, y^*, z^*]$ has the form

$$
J = \begin{pmatrix} 0 & -1 & -1 \\ 1 & a & 0 \\ z^* & 0 & x^* - c \end{pmatrix}.
$$

The nature of an equilibrium point depends on the eigenvalues of characteristic equation. This is now defined as $\det(J - \lambda I) = 0$. Then, the characteristic equation is given by

$$
\det \begin{pmatrix} -\lambda & -1 & -1 \\ 1 & a - \lambda & 0 \\ z^* & 0 & x^* - c - \lambda \end{pmatrix} = 0.
$$

The eigenvalues can be expressed as the roots of polynomial

$$
P(\lambda) = \lambda^3 + (c - a - x^*)\lambda^2 + (ax^* - ac + z^* + 1)\lambda + (c - x^* - az^*). \tag{3.5}
$$

The previous computation yields that two cases must be investigated, i.e. the cases when one and two fixed points exist.

3.2.1 The case of one equilibrium point

The Rössler system has only one equilibrium point if $c^2 = 4ab$. Thus, evaluating the Jacobian matrix at the fixed point $\mathbf{x}^*$ given by (3.4), the roots of characteristic polynomial (3.5) can be obtained from

$$
\lambda^3 + (\frac{c}{2} - a)\lambda^2 + (\frac{c}{2a} - \frac{ac}{2} + 1)\lambda = 0.
$$

Obviously, one eigenvalue is zero and the other two can be easily computed as the roots of quadratic equation

$$
\lambda^2 + (\frac{c}{2} - a)\lambda + (\frac{c}{2a} - \frac{ac}{2} + 1) = 0.
$$

Therefore, the eigenvalues of characteristic equation for $\mathbf{x}^* = \left[\frac{c}{2}, -\frac{c}{2a}, \frac{c}{2a}\right]$ are

$$
\lambda_1 = 0,
$$

$$
\lambda_{2,3} = \frac{a}{2} - \frac{c}{4} \pm \frac{1}{2}\sqrt{\left(\frac{c}{2} + a\right)^2 - \frac{2c}{a} - 4}.
$$

Since at least one of the eigenvalues has the zero real part, the fixed point is nonhyperbolic and thus difficult to classify. Analytical computation requires applying the theory given on the center manifold or finding Lyapunov function that would either confirm or disprove the stability of this equilibrium point. Such analysis will not be given here, however, classification of a single equilibrium point for the Rössler system was proposed in [20].

Following the analytical results from [20], the choice $a = 1$, $b = 10$ (hence $c = 2\sqrt{10}$) should classify the equilibrium point as a locally stable node. The results of a numerical experiment indicate, that the equilibrium point is truly locally stable as can be seen in Figure 3.1. However, the stability is secured only for a small basin of attraction. The basin of attraction of an equilibrium point represents a region in the phase space such that any trajectory starting in this region will be eventually attracted into this equilibrium point.

The reason, why the attracting region is small for this system is due to the significant sensitivity of the system in general. Thus, in Figure 3.1, the initial points were carefully chosen to fit in the corresponding region of attraction. On the other hand, Figure 3.2 shows the evolution of the system when the initial point is taken a bit further from the equilibrium point. Despite the fixed point being locally stable, it is no longer attracting the trajectory to itself. Furthermore, the trajectory escapes to infinity.

In both figures the equilibrium point is denoted by red star, and each initial point with a green cross. For this particular combination of parameters, the fixed point has coordinates $\mathbf{x}^* = [3.16, -3.16, 3.16]$. The initial point $\mathbf{x}_0 = [3.1, -3.1, 3]$ belongs to the basin of attraction, which means that the trajectory starting at this point will reach $\mathbf{x}^*$ as $t \to \infty$ (Figure 3.1). On the other hand, the trajectory starting at $\mathbf{x}_0 = [3.3, -2.4, 2.7]$ will be escaping to infinity with the spiral motion (Figure 3.2).
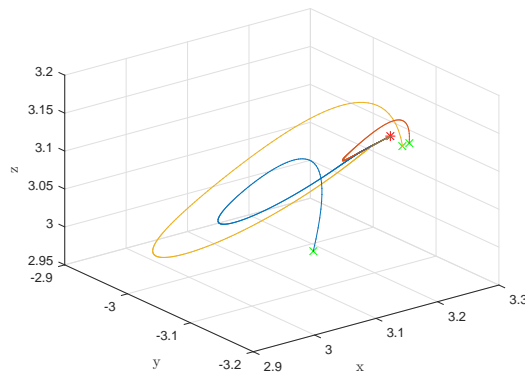

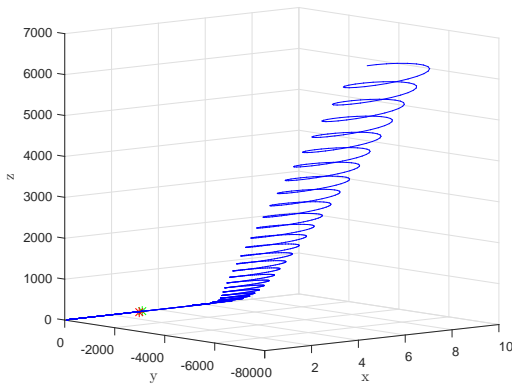Figure 3.1: $(a = 1, b = 10, c = 2\sqrt{10})$; $\mathbf{x}_0$ inside the basin of attraction.

Figure 3.2: $(a = 1, b = 10, c = 2\sqrt{10})$; $\mathbf{x}_0$ outside the basin of attraction.

3.2.2 The case of two equilibrium points

The system has two equilibrium points if the condition $c^2 > 4ab$ holds. Similarly to the previous case, the eigenvalues of characteristic equation (3.5) must be computed for both points $\mathbf{x}_1^*$ and $\mathbf{x}_2^*$. At this point, however, the task is to solve a general cubic equation which might be a bit complicated matter. One possibility is to apply the Cardan's method which gives the algorithm for finding eigenvalues of cubic function. Another approach consists of applying the Routh–Hurwitz criterion which was presented in Chapter 1.

Recall, the characteristic equation is given by (3.5). Then, according to Routh-Hurwitz criterion, all its roots are negative or have a negative real part if and only if all determinants of the Hurwitz matrices H_1, H_2, H_3 are positive. In this case it means, that all of the following conditions must hold

$$
\begin{aligned}
&\det H_1 = c - a - x^* > 0 \quad \text{and} \\
&\det H_2 = (c - a - x^*)(ax^* - ac + z^* + 1) - (c - x^* - az^*) > 0 \quad \text{and} \\
&\det H_3 = (c - x^* - az^*)[(c - a - x^*)(ax^* - ac + z^* + 1) - (c - x^* - az^*)] \\
&\qquad\ = (c - x^* - az^*)\det H_2 > 0.
\end{aligned}
\tag{3.6}
$$

Particularly, two cases must be investigated as there are two equilibrium points. In the sequel, each fixed point will be studied separately by fitting the values from (3.2) and (3.3) into (3.6).

Fixed point $\mathbf{x}_1^*$

In this case it is possible to start from the last determinant of (3.6) and focus on the condition $\det H_3 = (c - x^* - az^*)\det H_2 > 0$. Since it is desired that $\det H_2 > 0$, the second term in the inequality must be also positive, i.e. $(c - x^* - az^*) > 0$. However, substitution z^* and x^* with the values from (3.2) yields

$$
(c - x^* - az^*) = -\sqrt{c^2 - 4ab} < 0,
$$

which means that either $\det H_3 < 0$ or $\det H_2 < 0$. Therefore, the equilibrium point $\mathbf{x}_1^*$ is not stable for any combination of a, b, c.

Fixed point $\mathbf{x}_2^*$

The case of the second equilibrium point requires more computations. Unlike the previous case, here the term $(c - x^* - az^*) = \sqrt{c^2 - 4ab}$ is always positive as far as two equilibrium points exist and thus the condition for $\det H_3$ is satisfied if and only if $\det H_2 > 0$. From the first two equations of (3.6) follows: the roots of (3.5) have negative real parts if and only if

$$
\sqrt{c^2 - 4ab} > 2a - c \quad \text{and} \quad a(a - c)\sqrt{c^2 - 4ab} > ac(c - a) - 2(a^2b + b - a).
$$

These two inequalities give the desired conditions but they are still unwieldy in sense of expressing one of the parameters. More practical conditions were derived and proven in [21], [22].

Theorem 11. *The fixed point $\mathbf{x}_2^*$ is locally asymptotically stable if and only if parameters a, b, c satisfy:*

(i) *a, c belong to $S_1 \cup S_2$ given as*

$$S_1 = \{(a,c) : a \leq 1 \ and \ c > 2a\}, \tag{3.7}$$

$$S_2 = \{(a,c) : a \in (1, \sqrt{2}) \ and \ c \in (2a, 2a/(a^2 - 1))\}. \tag{3.8}$$

(ii) *b satisfies $b_H(a,c) \leq b < b_E(a,c)$, where*

$$b_H(a,c) = \frac{a(2 - a^4 + ca^3 + 2a^2 - ca + c^2 + (c-a)\sqrt{a^6 - 4a^4 + 2ca^3 - 4a^2 + c^2}}{2(a^2 + 1)^2},$$

$$b_E(a,c) = \frac{c^2}{4a}.$$

Proof. See [21]. □

To demonstrate the theoretical result given in the theorem, two different examples will be further presented with the value of parameter a from both of the sets S_1 given by (3.7) and S_2 given by (3.8). Firstly, assume $a \in S_1$, precisely the threshold case $a = 1$. In order to fulfil the condition $c > 2a$ the value of c is chosen as $c = 3$. By this choice, only a small interval of possible b is left. One of the possible values of b is $b = 2.22$. As can be observed from Figure 3.3a, under the choice of initial states (green stars) from the close neighbourhood of $\mathbf{x}_2^*$, the trajectories are attracted into this equilibrium point, particularly with a spiral movement. This illustrates that $\mathbf{x}_2^*$ is locally asymptotically stable. Similarly, Figure 3.3b shows the attraction of another stable equilibrium when $a \in S_2$. In this second case, the combination of parameters was chosen as $a = 1.3$, $b = 1.7306$, $c = 3$.
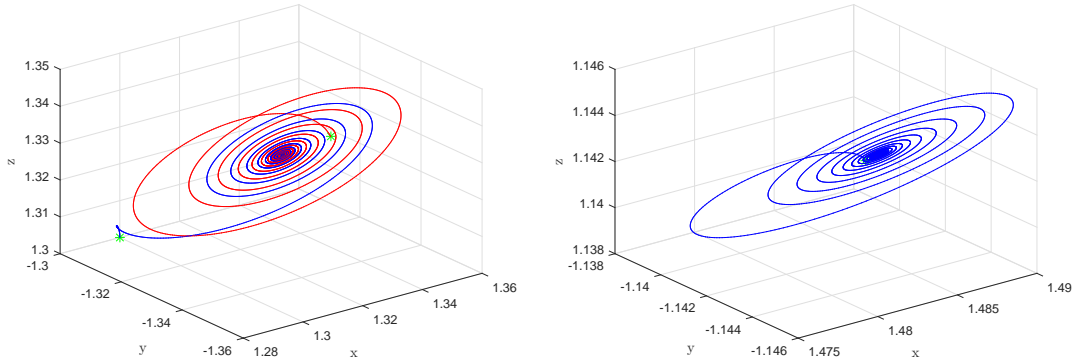
(a) $a \in S_1$, $\mathbf{x}_0 = [1.3, -1.3, 1.3]$.　　　(b) $a \in S_2$, $\mathbf{x}_0 = [1.485, -1.142, 1.142]$.

Figure 3.3: Demonstration of stable fixed points.

Even though the attraction of these fixed points was illustrated, both of the presented cases have small basin of attraction. Similarly to the case of one equilibrium, the initial points were carefully chosen to fit in the corresponding region of attraction.

In Figure 3.4, the same parameters as in Figure 3.3a were used, with only difference in the starting point. Again, the attraction towards the fixed point failed when the starting point was chosen a bit further from $\mathbf{x}_2^*$.

Another consequence of Theorem 11 is that any choice of parameters will never lead to a system with asymptotically stable equilibrium point whenever $a \geq \sqrt{2}$.
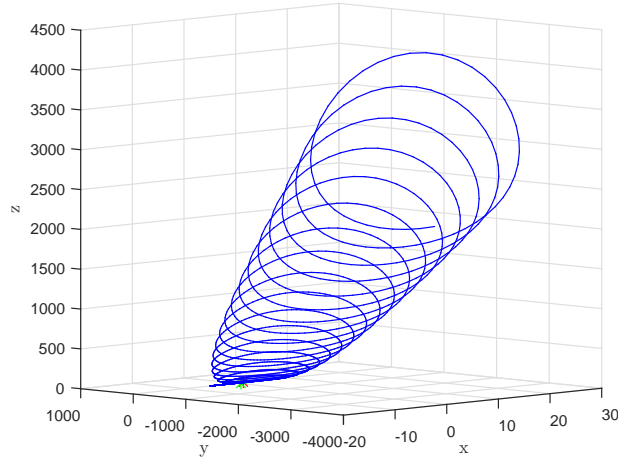
Figure 3.4: $a \in S_2$, $\mathbf{x}_0 = [0.8, 1, 0.6]$.

3.3   Numerical Analysis for varying c

In general, investigating analytically nonlinear systems with multiple parameters is a demanding task to do, and this is also the case of the Rössler model. Therefore, numerical methods must be often used. Fixing one or two parameters and letting the rest of them vary, one can considerably simplify the analysis. Following the Rössler's original work, a and b will be considered as fixed parameters and c will vary as a bifurcation parameter. Suppose

$$a = b = 0.1$$
$$\Rightarrow c \geq \sqrt{4ab} = 0.2.$$

According to Routh–Hurwitz criterion, in all cases when $a = b$, no possible value of c exists for which the equilibrium point $\mathbf{x}_2^*$ is asymptotically stable. Thus, analysis of other specific solutions can be performed.

Consider the Rössler system given by (3.1) with parameters $a = b = 0.1$, $c \in [0.2, 20]$ and with initial condition $\mathbf{x}_0 = [1, -1, 0]$. Firstly, assume $c = 0.2$. This case corresponds to the situation when only one fixed point exists. Moreover, this value of c is critical for the system ($c = c_{cr}$), since the system undergoes so-called fold bifurcation (saddle-node bifurcation) as c decreases or increases. During fold bifurcation, the single fixed point either disappears (if $c < c_{cr}$), or two equilibrium points are formed from the single fixed point (if $c > c_{cr}$), either one stable and one unstable, or two unstable.

The case of one equilibrium was already discussed in the beginning of this chapter. It was shown that the corresponding fixed point is nonhyperbolic, and for the initial value chosen for this analysis the behaviour is plotted in Figure 3.5. The trajectory starting at $\mathbf{x}_0$ is moving fast away from the fixed point with a spiral movement.

Greater interest arises in the cases of two equilibria. For any $c > c_{cr} = 0.2$, two equilibria exist. Moreover, for this specific choice of parameters a, b, a stable limit cycle is created immediately when the parameter c is increased above 0.2. However, the formation of the stable limit cycle comes from a bifurcation over a different system parameter as is described in [20]. The stable cycle has a great effect on the system as all the trajectories

starting in its neighbourhood will converge to this cycle as $t \to \infty$. On the contrary to the cases of stable equilibrium points, the basin of attraction of this orbit is significantly larger. Moreover, this limit cycle plays the main role in the transition to chaos via period doubling bifurcation. This phenomenon is based on a sequence of actions when the period of the limit cycle is doubled, leading to a loss of stability and chaotic behaviour. The transition to chaos and back to periodicity is described in the next part.
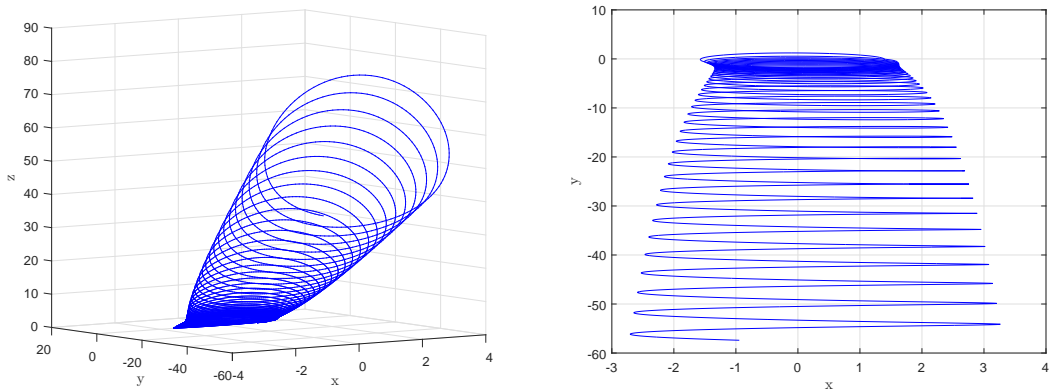

Figure 3.5: Bifurcation analysis: $c = 0.2$; critical value.

At first, the creation of stable limit cycle can be observed in Figure 3.6. For a demonstration, two starting points were chosen, one from 'outside' and one from 'inside' of the assumed position of the limit cycle. The figure provides a good idea where the actual orbit is located. Since the limit cycle is of period one, it is often called period one orbit. This terminology will be useful later when cycles of different period appear.
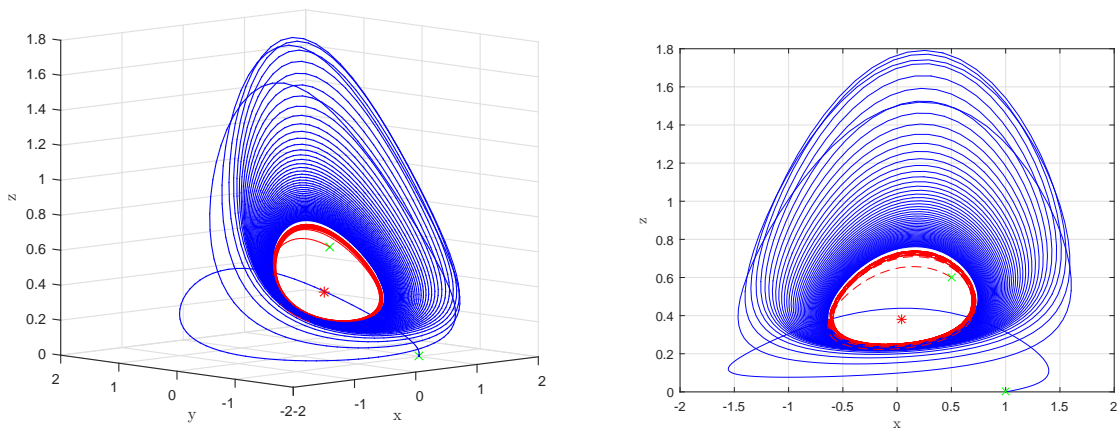

Figure 3.6: Bifurcation analysis: $c = 0.21$; demonstration of limit cycle.

Further increasing values of parameter c will not bring any new observation for a while, since up to the value $c \approx 5.3$ the behaviour of the system has the same scenario. All nearby trajectories settle down on the period one orbit as can be seen in Figure 3.7 which was plotted for the value $c = 4$. The 2D view shows the settled solution on the periodic orbit.
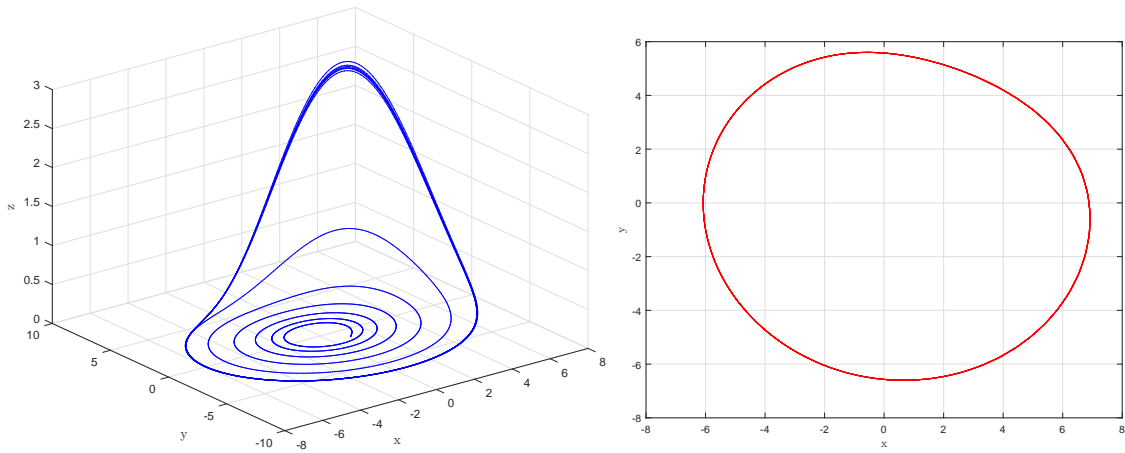
Figure 3.7: Bifurcation analysis: $c = 4$; period one orbit.

Once c passes the value 5.3, the system undergoes first period doubling. The periodic orbit enlarges its period twice from the original value. The new limit cycle has period two and it is made of two loops. A demonstration of period two orbit is depicted in Figure 3.8 for the value $c = 5.4$. The period two orbit occurs up to the value $c \approx 7.8$ when another period doubling takes place.
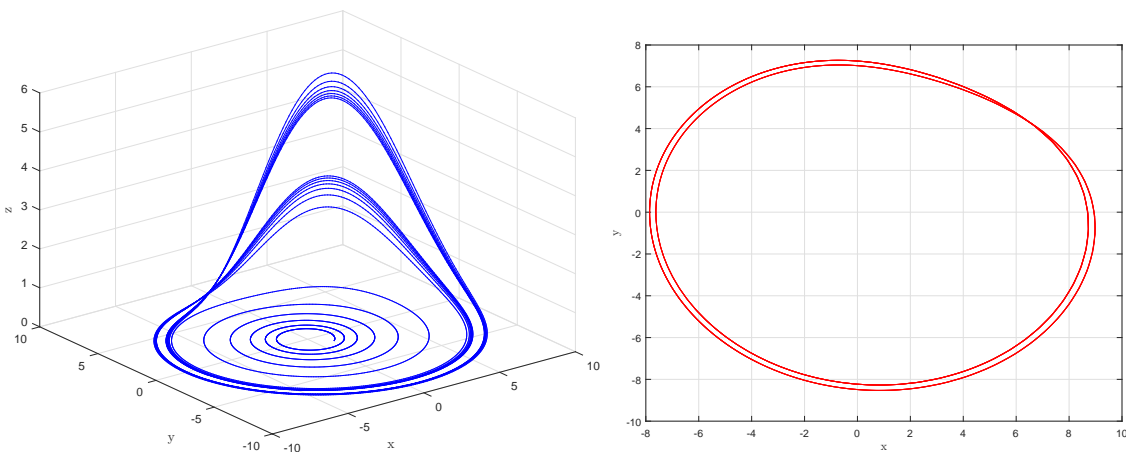

Figure 3.8: Bifurcation analysis: $c = 5.4$; period two orbit.

In the interval between the values 7.8 and 8.6, period four orbits can be observed as is in Figure 3.9, following another period doubling. Around the value $c \approx 8.7$, period eight orbit appears. With further increase of the value of c the period doubling happens so often, that it starts to lead to chaos which appears already around the value $c \approx 9$. Figure 3.10 shows the chaotic behaviour of the system for the value $c = 10$. The solution will never settle down as new and new loops are created. This can be observed from the 2D view which shows evolution for $t >> t_0$.

This phenomenon continues up to the value $c \approx 11.9$. At this value a collapse of chaos appears suddenly and the periodicity of the solution reappears. For the interval between the values 11.9 and 12.5, the solution settles onto period three orbit as can be seen in Figure 3.11a for $c = 12$. At the value 12.6, the period doubling bifurcation occurs

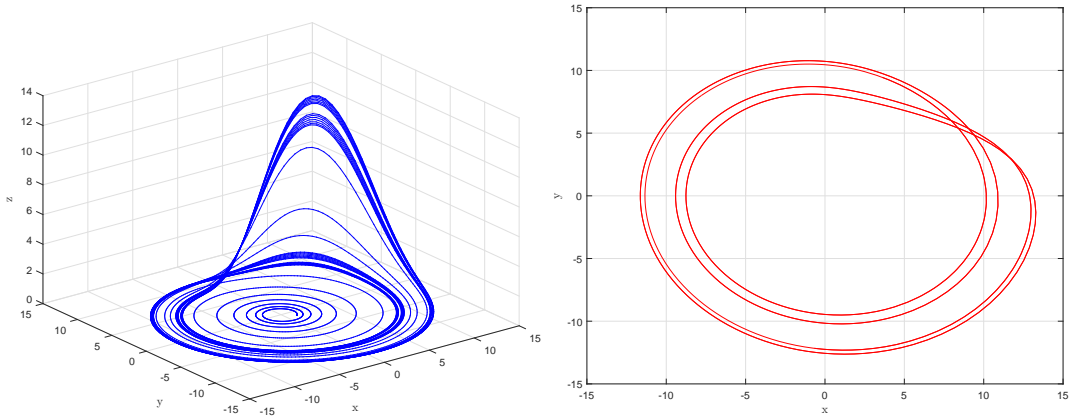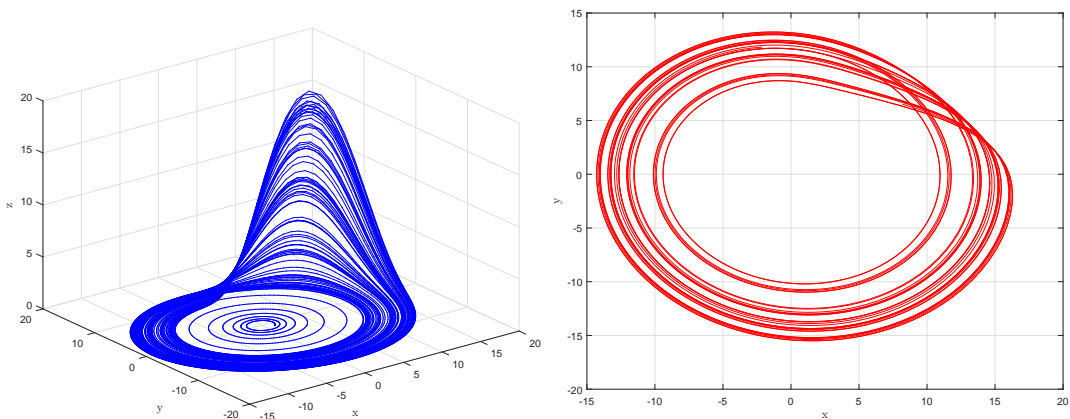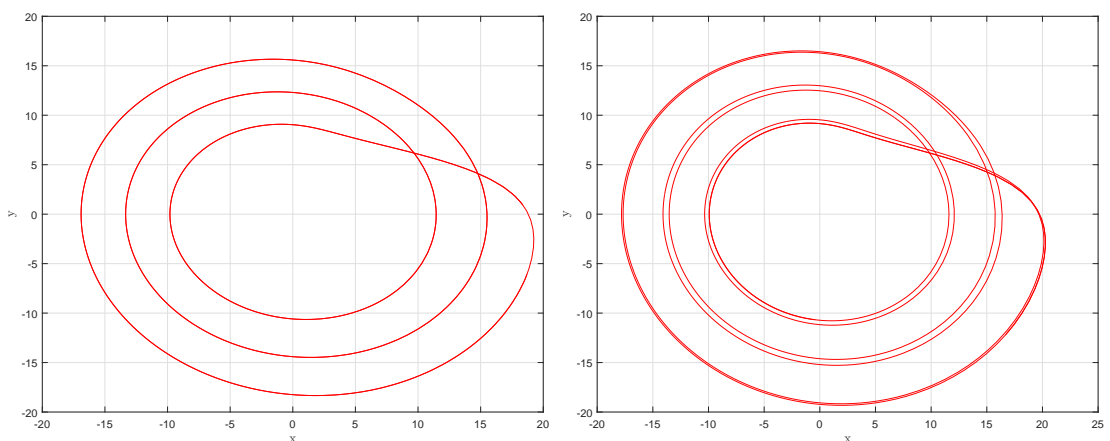Figure 3.9: Bifurcation analysis: $c = 8$; period four orbit.

Figure 3.10: Bifurcation analysis: $c = 10$; chaotic behaviour.

again letting the period enlarge to six. The six period orbit can be seen in Figure 3.11b representing the settled solution for the value of $c = 12.5$.

(a) $c = 12$; period three orbit.

(b) $c = 12.7$; period six orbit.

Figure 3.11: Bifurcation analysis: $c = 12$; $c = 12.7$.

The trajectory for the value $c = 13$ in Figure 3.12 is already chaotic and chaos occurs for increasing c up to the value 15.4, where the solution becomes periodic again, however, just for a small interval of c. The collapse of chaos for a small interval of the bifurcation parameter is often called a periodic window, precisely period five window in this case (see Figure 3.13). Finally, starting with the value 15.5 till the end of the investigation at $c = 20$, the behaviour is fully chaotic as is noticeable in Figure 3.14.
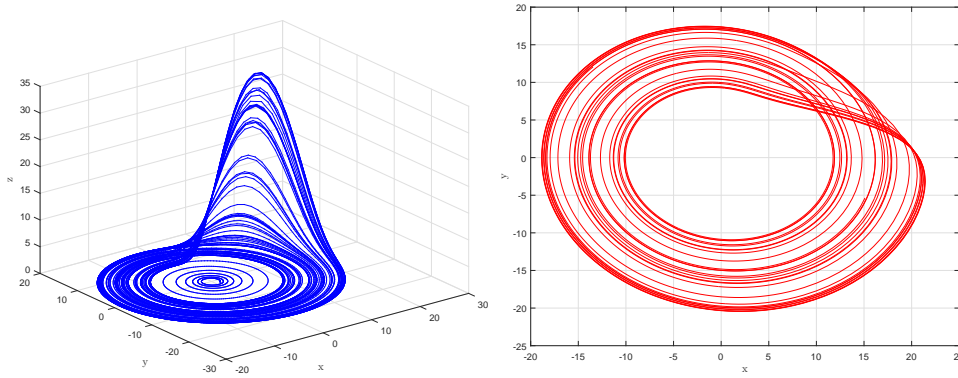

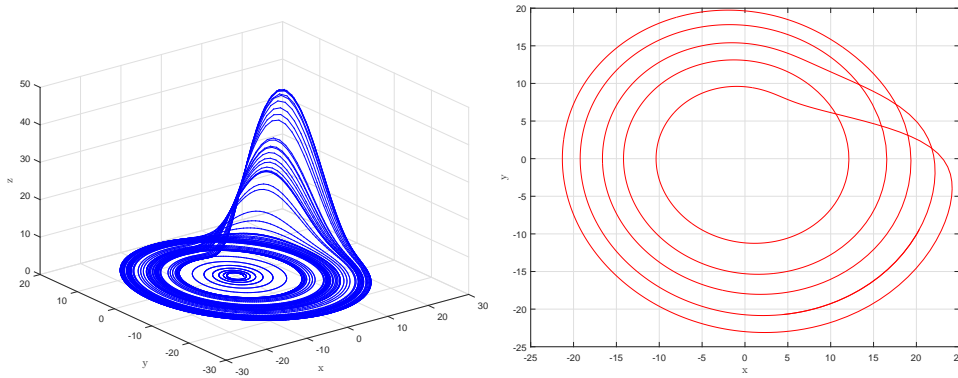Figure 3.12: Bifurcation analysis: $c = 13.5$; chaotic behaviour.

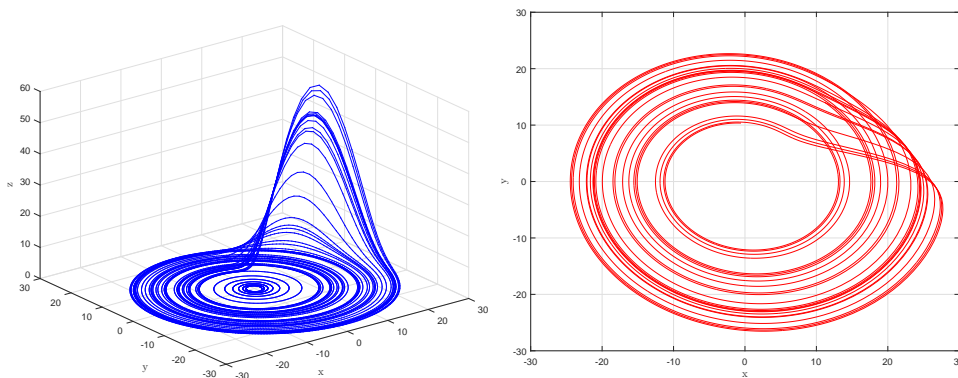Figure 3.13: Bifurcation analysis: $c = 15.4$; collapse of chaos.

Figure 3.14: Bifurcation analysis: $c = 18$; chaotic behaviour.

Bifurcation diagram

It is apparent, that the method used above is not very practical, since every value of c from the chosen interval must be separately plotted and investigated. In case, when the only desired information is whether the chaos occurs or not for certain values, a bifurcation diagram can be plotted using Poincaré theorem.

Creation of a bifurcation diagram is based on the idea similar to the construction of Poincaré map. The nature of any structure in dynamical systems is determined by the behaviour of the system in its neighbourhood as time goes to infinity. Obviously, it is impossible to run such calculation. Therefore, sufficiently long time $t = T_s$ is chosen after which the system is assumed to behave as it would behave in infinity. Clearly, this can be claimed only if the solution approaches an attracting fixed point or an attracting periodic orbit. In case of stable periodic orbits, it can be assumed that for time $t > T_s$, if the trajectory runs through a certain point in the phase space, then after time equal to the period of the orbit, the trajectory will cross this point again. Moreover, this behaviour will be repeated infinitely.

Suppose, that the local maxima of one state variable are measured and recorded in the graph for a certain period of time starting at some $t > T_s$. Then, if the solution of the system is attracted to a periodic orbit, all the measurements coincide at one value. However, in the case when chaos occurs in the system, the measurements will differ. The bifurcation diagram can be then explained as follows. For each value of bifurcation parameter, the number of different values recorded in the graph corresponds to the periodicity of the limit cycle. Thus, in the case of period one orbit, only a single value of the measured state variable will occur in the graph. On the contrary, if for certain parameters the system is chaotic, then there will be infinitely many different values plotted in the graph.
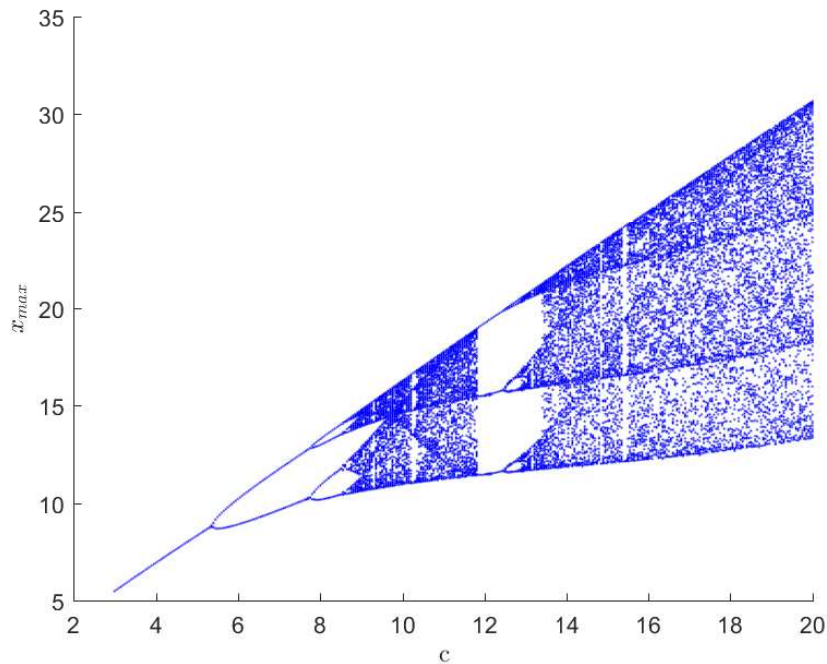
Figure 3.15: Bifurcation diagram for varying c.

The bifurcation diagram depicted in Figure 3.15 confirms the results of the numerical analysis done before. Clearly, for small c, period one orbit occurs, following several period doubling. Around the value $c = 9$ there is already too many points plotted in the figure. This suggests the transition to chaos. The region from 9 to 12 is clearly chaotic and similarly the region from 13 till the end of the investigated interval of the bifurcation parameter (except of the small interval around 15.4 which refers to periodic window). Matlab code for the bifurcation diagram was inspired by [23].

4 CONTROLLING CHAOS

The impossible long-term prediction and sensitivity on the initial data had been the reason why the chaotic systems were undervalued and undesired in the past. The strange behaviour had often been attributed to random influences and thus, there was a tendency to avoid such systems or to design them out if possible. However, with the development in the computer science, the potential usefulness of chaotic systems have been found, followed by an idea of stabilizing (control) such systems in the early '90s.

The concept of stabilization usually includes an implementation of external forces (perturbations) to make the system behave as desired. That means reaching a chosen state and secure that the system becomes stable at this state and even more, resistant to another perturbations. For this task, the properties of chaotic systems can be beneficial, since these systems are also extremely sensitive to the effect of perturbation. Under certain conditions, it is then possible to find suitable perturbation parameters to control the system. On the other hand, the goal of control does not have to always implement stabilization of a chosen system. The control can be as well used in the opposite way, making the trajectories become chaotic. [7], [11], [24]

In this chapter, some of the well-known methods will be presented, following deeper investigation in the time-delayed feedback control method, where several examples will be introduced.

4.1 Methods of control

There are two main approaches to achieve a certain control over the system. The first approach is based on application of a feedback process, e.g. external force, that influences the trajectory to the desired direction. Hence, the actual state of the system must be monitored during all the control process. Into this category belong the OGY method, the external force control with continuous-time or the Pyragas method (time-delayed feedback control method). The second group represents the nonfeedback methods. Such methods do not need monitoring of trajectories and so they can be applied at any time. On the other hand, nonfeedback methods usually affect more the system itself.

4.1.1 OGY Method

The OGY method was firstly introduced in 1990 and it was named after its inventors Q. Ott, C. Grebogi and J. A. Yorke. The method is based on elimination of chaos by applying small time-dependent perturbations. [25] The method takes advantage of the properties of chaotic attractors, precisely that a chaotic attractor contains within it an infinite number of unstable periodic orbits of all periods. The target of the control is to apply the force in appropriate time to direct the trajectory on one of those unstable orbits, where it remains. The first step is choosing one of the orbits, and computing precisely the perturbation needed. The perturbation, which is usually very small, is then applied on the system whenever the trajectory is close to this chosen orbit. This way, the trajectory is getting closer with each perturbation up to the point when it stays on the orbit and thus the orbit becomes stable. In some papers, this process is described as suppressing chaos by shadowing one the system's unstable periodic orbit. [11]

The OGY method belongs to the feedback control group with non-invasive control. The non-invasive control means that the control vanishes once the stability is achieved. The method is very general and can be used for stabilizing both periodic orbits or steady states inside the chaotic attractor. The advantage of OGY method is that, it is sufficient to study only part of the chaotic model, i.e. the Poincaré map. On the other hand, the method requires a permanent tracking of the state of the system and a lot of computation to earn the precise perturbations necessary to stabilize the system.

4.1.2 Time-Delayed Feedback Control

The method of time-delayed feedback control (TDFC), also called time-delayed auto synchronization, was originally introduced by K. Pyragas in 1992 to stabilize unstable periodic orbits [26]. Unlike the OGY method, TDFC uses time-continuous perturbation and thus can avoid some problems connected with OGY method. Moreover, the method does not need any external source of perturbation since the control force is constructed from the delayed output signal applied in a special form in the system input. This way a certain self-control of the system is achieved. Hence, the main task in this method is to construct the form of the perturbation which will stabilize the system but will not change the solution. To construct the form of control, recall, an autonomous nonlinear dynamical system

$$\mathbf{x}'(t) = f(\mathbf{x}(t)), \tag{4.1}$$

where $\mathbf{x} \in \mathbb{R}^n$, and $f : \mathbb{R}^n \to \mathbb{R}^n$ is a function defined as $f : \mathbf{x} \to f(\mathbf{x})$. In general, a system under some control force can be written as

$$\mathbf{x}'(t) = f(\mathbf{x}(t)) + u(t). \tag{4.2}$$

Suppose now the system is 1D, i.e. given by single equation $x' = f(x)$. Let $\tau \in \mathbb{R}^+$ be the time delay and $K \in \mathbb{R}$ the control gain (weight of the feedback force), then according to the Pyragas scheme, the control force is constructed from the difference of the present state $x(t)$ and its delayed value $x(t - \tau)$. In other words, the perturbation is of the form

$$u(t) = K[x(t - \tau) - x(t)].$$

The advantage of the delay arise from the property of the periodic orbits, such that, if τ is equal to the period of the orbit ($\tau = T$) then the control force vanishes if the orbit is stabilized since $x(t+T) = x(t)$. Thus, the method is non-invasive. Equivalently, it can be shown, that the non-invasive property holds also for stabilizing steady states. The force vanishes when the steady state x^* is stabilized as $x^*(t) \equiv x^*(t-\tau)$. However, the optimal choice of the time delay is not so obvious in this case.

The TDFC method is easy to implement, however, the crucial task is finding a suitable combination of parameters τ and K which makes the stabilization successful. Later in this chapter, an assertion will be presented, giving restrictions on the possible choice of the pairs ($[K, \tau]$ for the Pyragas scheme with diagonal feedback control, i.e. when the matrix describing the control is diagonal. The controlled system (4.2) in the case of Pyragas scheme has the form

$$\mathbf{x}'(t) = f(\mathbf{x}(t)) - KI[\mathbf{x}(t) - \mathbf{x}(t - \tau)], \tag{4.3}$$

where I is an identity matrix.

4.1.3 Non-Feedback methods

As it was mentioned in the beginning of this chapter, one possibility to avoid chaos is to design it out from the system. The idea of this method can be demonstrated on the dynamical vibration absorber. The absorber is a small mass connected to the main system preventing the system to reach resonance frequency. Similarly in controlling chaos, the considered system can be coupled with additional, much simpler system, that helps it to avoid chaotic behaviour.

4.2 Applying the Time-Delayed Feedback Control

This part of the work is focused on the TDFC method presented earlier. Firstly, the method will be demonstrated on a simple 2D example, which was studied in the work of P. Hövel [27]. Then, a general assertion will be stated, presenting different approach of finding suitable pairs $[K, \tau]$ for successful stabilization. The 2D example will be then used again, to demonstrate the second approach. Finally, the task of stabilizing the chaotic Rössler system will be presented.

4.2.1 Stabilization of Unstable Focus

Both periodic orbits and fixed points can be stabilize by the TDFC method. Thus, an example of unstable focus in $\mathbb{R}^2$ is chosen to demonstrate the method. This task is described in more details in Chapter 3.2 from [27]. A brief summary of the results from [27] will be presented as it will be useful in the next considerations. Suppose a linear dynamical system in $\mathbb{R}^2$ of the form

$$\mathbf{x}'(t) = \begin{pmatrix} a & b \\ -b & a \end{pmatrix} \mathbf{x}(t), \tag{4.4}$$

where $a, b \in \mathbb{R} \smallsetminus \{0\}$ are two different constants. Besides that, if $a > 0$, then eigenvalues λ of the characteristic equation are complex with $\Re(\lambda) > 0$. The system exhibits unstable focus in the origin. Furthermore, if $\mathbf{x}_0$ is the initial point, then solution of this system is given by

$$\mathbf{x}(t) = e^{at} \begin{pmatrix} \cos(bt) & \sin(bt) \\ -\sin(bt) & \cos(bt) \end{pmatrix} \mathbf{x}_0.$$

Assuming the Pyragas scheme given by (4.3), the system (4.4) under the time-delayed feedback control becomes

$$\mathbf{x}'(t) = \begin{pmatrix} a & b \\ -b & a \end{pmatrix} \mathbf{x}(t) - KI[\mathbf{x}(t) - \mathbf{x}(t - \tau)]. \tag{4.5}$$

It is easily seen that in the absence of control, i.e. $K = 0$, the system gets back into (4.4). The stabilization process is successful if there exists a suitable choice (or choices) of $[K, \tau]$ for which the origin becomes asymptotically stable, i.e. all eigenvalues s of the characteristic equation of system given by (4.5) satisfy $\Re(s) < 0$. Thus, it is necessary to prescribe the restrictions on the control gain K and time delay τ to obtain the domain of control. This leads to the following computation.

In the first step, eigenvalues s_i corresponding to the fixed point in the origin need to be obtained from the characteristic equation. Using the exponential ansatz for $\mathbf{x}(t)$, the characteristic equation of (4.5) is given as

$$0 = \det \left[\begin{pmatrix} a - s & b \\ -b & a - s \end{pmatrix} - K \begin{pmatrix} 1 - e^{-s\tau} & 0 \\ 0 & 1 - e^{-s\tau} \end{pmatrix} \right],$$

which after the computation yields

$$a \pm \mathrm{i}b = s + K(1 - e^{-s\tau}). \tag{4.6}$$

As mentioned earlier, system is asymptotically stable, if for all s is $\Re(s) < 0$. Therefore, it is convenient to find the threshold of stability, i.e. $\Re(s) = 0$. For easier manipulation, s is written as a complex number, $s = p + \mathrm{i}q$. Using the Euler's formula

$$e^{-s\tau} = e^{-p\tau}(\cos(q\tau) - \mathrm{i}\sin(q\tau)),$$

the equation (4.6) can be divided in real and imaginary part as

$$a = p + K[1 - e^{-p\tau}\cos(q\tau)],$$
$$b = q + Ke^{-p\tau}\sin(q\tau).$$

The threshold between stability and instability in complex plane is given by $p = 0$. Allowing $p = 0$, the system gets easier into

$$a = K - K\cos(q\tau), \tag{4.7}$$
$$b = q + K\sin(q\tau). \tag{4.8}$$

From the range of cosine function, it is easy to see that a lower bound for the control gain K providing successful stabilization is obtained from (4.7) and given by

$$\frac{a}{2} \leq K.$$

Further, using the trigonometrical identities, the equations (4.7) and (4.8) written as

$$\frac{K - a}{K} = \cos(q\tau),$$
$$\frac{b - q}{K} = \sin(q\tau),$$

can be put to the second power and sum together, leading into

$$\left(\frac{K - a}{K}\right)^2 + \left(\frac{b - q}{K}\right)^2 = \cos^2(q\tau) + \sin^2(q\tau) = 1. \tag{4.9}$$

The equation (4.9) enables to express q

$$\frac{b - q}{K} = \pm\sqrt{1 - \left(\frac{K - a}{K}\right)^2}$$
$$\Rightarrow q = b \mp \sqrt{(2K - a)a}. \tag{4.10}$$

Substituting q from (4.10) into the equation (4.7), the time delay τ can be obtained as a function of the control gain K

$$\frac{K - a}{K} = \cos((b \mp \sqrt{(2K - a)a})\tau)$$

$$\Rightarrow \tau(K) = \frac{\arccos\left(\frac{K-a}{K}\right)}{b \mp \sqrt{(2K - a)a}}. \tag{4.11}$$

However, the solution obtained by (4.11) is given only on the interval where cosine function is a bijection. Thus, extending the interval according to the periodicity of the cosine function, three families of branches of solutions are obtained. Namely, let n be a non-negative integer and suppose firstly $q = b - \sqrt{(2K - a)a}$. Taking into account the condition of non-zero denominator ($K \neq \frac{a^2+b^2}{2a}$), two families of branches arise

$$\tau_1(K, n) = \frac{2n\pi + \arccos\left(\frac{K-a}{K}\right)}{b - \sqrt{(2K - a)a}}, \qquad \frac{a}{2} \leq K < \frac{a^2 + b^2}{2a}, \tag{4.12}$$

$$\tau_2(K, n) = \frac{(2n + 1)\pi - \arccos\left(\frac{K-a}{K}\right)}{-b + \sqrt{(2K - a)a}}, \qquad \frac{a^2 + b^2}{2a} < K. \tag{4.13}$$

Finally, for $q = b + \sqrt{(2K - a)a}$ the denominator is always non-zero and the time delay is given as

$$\tau_3(K, n) = \frac{(2n + 1)\pi - \arccos\left(\frac{K-a}{K}\right)}{b + \sqrt{(2K - a)a}}, \qquad \frac{a}{2} \leq K. \tag{4.14}$$

The region of suitable choices of parameters K and τ for which unstable focus can be stabilized is defined by the union of all subregions restricted by branches τ_1, given by (4.12), from bellow and τ_3, given by (4.14), from above for $n = 0, 1, 2, \ldots$. The family of branches τ_2 given by (4.13) are not relevant since $\tau_2 > \tau_3$ for all $K > \frac{a^2+b^2}{2a}$. To demonstrate the theoretical results, the parameters of the dynamical system (4.4) are fixed as $a = 0.1$ and $b = \pi$. The system has the form

$$\mathbf{x}'(t) = \begin{pmatrix} 0.1 & \pi \\ -\pi & 0.1 \end{pmatrix} \mathbf{x}(t). \tag{4.15}$$

According to the conditions given in (4.12) and (4.14), the domain of control for the system (4.15) is depicted in Figure 4.1. Particularly, subregions S_0, S_1, S_2, S_3 corresponding to $n = \{0, 1, 2, 3\}$ are presented. The red and blue curves correspond to the solutions of $\tau_1(K, n)$ and $\tau_3(K, n)$, respectively. It is easy to observe, that the number of suitable pairs $[K, \tau]$ decreases as the time delay increases.

The original uncontrolled system (4.15) is given in Figure 4.2a. On the other hand, Figure 4.2b refers already to a stabilized system, in this case with $[K, \tau] = [0.8, 1.5]$ from the subregion S_0. The fixed point is stabilized and the trajectory approaches $\mathbf{x}^*$ as $t \to \infty$. On the contrary, choosing parameters outside the domain of control will not stabilize the fixed point and the trajectory will escape to infinity. Figure 4.2c represents the choice of parameters $[K, \tau] = [1.5, 2]$ under which it is not possible to stabilize the fixed point. Due to the numerical method which was used for the feedback control schemes, the trajectory is firstly getting closer to the fixed point, however, it soon reverses the direction. The

fixed point remained unstable as was expected. Finally, the choice of the values from the boundary of the subregions leads to a creation of a stable limit cycle. This phenomenon can be observed in Figure 4.2d. In this particular case K was fixed at the value $K = 1$ and τ was computed from the relation (4.12).

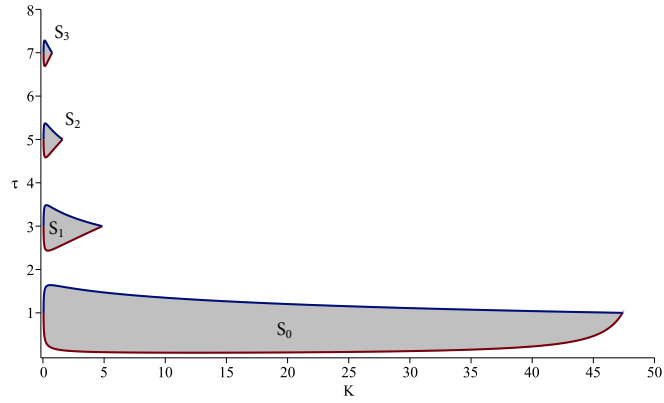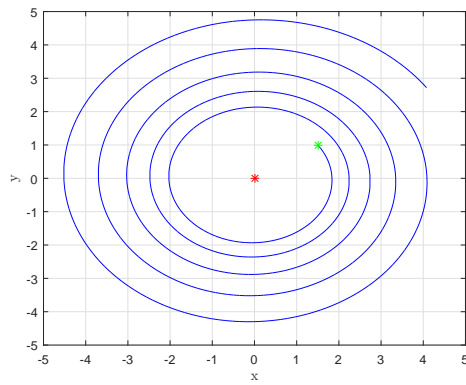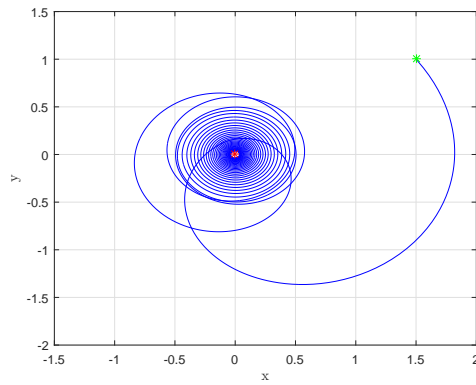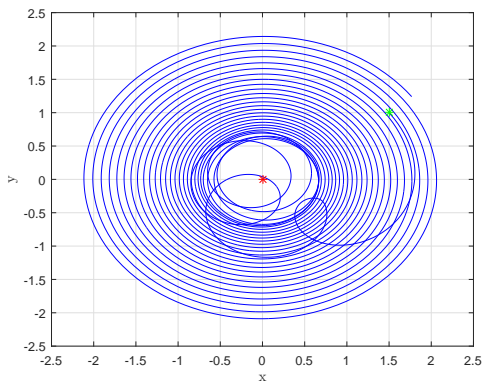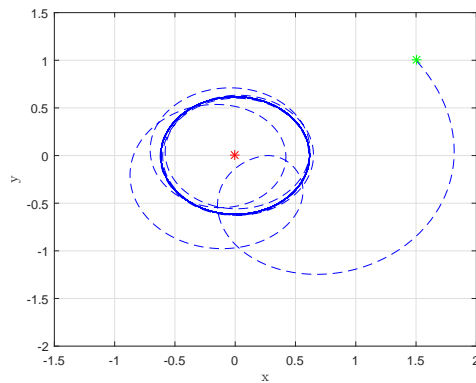Figure 4.1: Domain of control in (K, τ)-plane.

(a) Original system.

(b) $[K, \tau] = [0.8, 1.5]$; stabilized.

(c) $[K, \tau] = [1.5, 2]$; not stabilized.

(d) $[K, \tau] = [1, 1.63024]$; periodic orbit.

Figure 4.2: Stabilization of unstable focus.

4.2.2   General condition for finding domain of control

In the previous example, the stabilization via TDFC method was demonstrated for a particular case in 2D. The presented approach gives the condition for successful stabilization, however, it is not general enough. In the sequel, another approach will be introduced, providing more general method for obtaining the domain of control parameters.

Suppose the system (4.1) under the control of Pyragas type, i.e. system given by (4.3). The problem of stabilization of a fixed point can be determined by investigating the linearized controlled system around the equilibrium point. The linearization of (4.3) yields

$$\mathbf{x}'(t) = B\mathbf{x}(t) + KI\mathbf{x}(t - \tau), \tag{4.16}$$

where $\mathbf{x} \in \mathbb{R}^n$, the matrix $B \in \mathbb{R}^{n \times n}$ is given as $B = Df(\mathbf{x}^*) - KI$, where $Df(\mathbf{x}^*)$ is the Jacobian matrix of the original uncontrolled system (4.1) evaluated at the equilibrium point $\mathbf{x}^*$. The set of suitable control parameters $[K, \tau]$ is characterized by the following

Theorem 12. *Let $B \in \mathbb{R}^{n \times n}$ be matrix with eigenvalues λ_i, $i = 1, \ldots, n$ and let $K \in \mathbb{R}$, $\tau \in \mathbb{R}^+$. The zero solution of (4.16) is asymptotically stable if and only if each λ_i, $i = 1, \ldots, n$ satisfies any of the following conditions:*
  (i) $\Re(\lambda_i) + |K| < 0$ *and* τ *is arbitrary;*
  (ii) $\Re(\lambda_i) + |K| = 0$, $K \neq 0$ *and* $\tau\Im(\lambda_i) - \arg(K) \neq 2\ell\pi$ *for any $\ell \in \mathbb{Z}$;*
  (iii) $|\Re(\lambda_i)| - |K| < 0$
    and $\tau\sqrt{K^2 - (\Re(\lambda_i))^2} + \arccos\left(\frac{-\Re(\lambda_i)}{|K|}\right) < \arccos[\text{sgn}(K)\cos(\tau\Im(\lambda_i))]$.

Proof. To prove Theorem 12, it is necessary to show that the conditions presented in the assertion are necessary and sufficient for characteristic equation of (4.16) to have all eigenvalues with negative real part. Using the exponential ansatz for $\mathbf{x}(t)$, the characteristic equation has the form

$$\det\left[sI - B - KIe^{-s\tau}\right] = 0.$$

As the matrix B can be decomposed into the diagonal matrix with eigenvalues λ_i of B on its diagonal, it is possible to say that the equilibrium point $\mathbf{x}^*$ of (4.16) is asymptotically stable if and only if all roots of quasi-polynomial

$$F(s) = \prod_{i=1}^{n}(s - \lambda_i - Ke^{-s\tau})$$

have negative real part, i.e. $\Re(s) < 0$. Thus, it is possible to reduce the investigation on the roots of

$$s - \lambda_i - Ke^{-s\tau} = 0 \tag{4.17}$$

for each eigenvalue λ_i. Now, turning back to the conditions presented in the assertion, the goal is to show that all the roots s have negative real parts if and only if just one of the conditions (i)–(iii) holds.

Firstly, write λ instead of λ_i in (4.17) and express it from (4.17) as $\lambda = s - Ke^{-s\tau}$. Suppose a set defined as

$$U(K, \tau) = \{s - Ke^{-s\tau} : s \in \mathbb{C}, \Re(s) \geq 0\},$$

then on the contrary the property of stability is true if and only if $\lambda \notin U(K, \tau)$. Thus, it is enough to describe the structure of $U(K, \tau)$ for $K \neq 0$ and $\tau > 0$ (the case $K = 0$ is trivial). Since

$$s + Ke^{-\tau s} = s + Ke^{-\tau s}e^{i\pi}$$
$$= s - i\pi/\tau - Ke^{-\tau(s - i\pi/\tau)} + i\pi/\tau,$$

the set $U(-K, \tau)$ can be obtained from $U(K, \tau)$ via shifting by $i\pi/\tau$ along the imaginary axis. Thus, it is enough to restrict the investigation for $K > 0$. Using the properties from complex analysis, let $\hat{s}$, $-\pi < \tau\Im(\hat{s}) \leq \pi$ be such that $s = \hat{s} + i\,2\pi\ell/\tau$ for a suitable $\ell \in \mathbb{Z}$. Then

$$s - Ke^{-s\tau} = \hat{s} - Ke^{-\tau\hat{s}} + i\,2\pi\ell/\tau,$$

hence it is possible to consider another restriction of $U(K, \tau)$, namely to

$$U_0(K, \tau) = \{s - Ke^{-s\tau} : s \in \mathbb{C},\ \Re(s) \geq 0,\ -\pi/\tau < \Im(s) \leq \pi/\tau\}.$$

Finally, separating the real and imaginary part of (4.17), one can easily check that s^* is a root of (4.17) if and only if its complex conjugate $\overline{s^*}$ is the root of

$$s - \overline{\lambda} - Ke^{-s\tau} = 0,$$

$\overline{\lambda}$ being complex conjugate to λ. Consequently, because of symmetry of $U_0(K, \tau)$ with respect to the real axis, it is sufficient to describe the structure of the set

$$U_0^+(K, \tau) = \{s - Ke^{-s\tau} : s \in \mathbb{C},\ \Re(s) \geq 0,\ 0 \leq \Im(s) \leq \pi/\tau\}.$$

The border of $U_0^*(K, \tau)$ is formed by the sets

$$B_1(K, \tau) = \{s - Ke^{-s\tau} : s \in \mathbb{C},\ \Re(s) \geq 0,\ \Im(s) = \pi/\tau\},$$
$$B_2(K, \tau) = \{s - Ke^{-s\tau} : s \in \mathbb{C},\ \Re(s) = 0,\ 0 \leq \Im(s) \leq \pi/\tau\},$$
$$B_3(K, \tau) = \{s - Ke^{-s\tau} : s \in \mathbb{C},\ \Re(s) \geq 0,\ \Im(s) = 0\}.$$

Let $\lambda = \alpha + i\beta$. For $B_1(K, \tau)$, where $\beta = \pi/\tau$ it holds

$$B_1(K, \tau) = \{\alpha + i\pi/\tau - Ke^{-\tau\alpha - i\pi} : \alpha \in \mathbb{R},\ \alpha \geq 0\}$$
$$= \{\alpha + Ke^{-\tau\alpha} + i\pi/\tau : \alpha \in \mathbb{R},\ \alpha \geq 0\}.$$

Since $f_1(\alpha) = \alpha + Ke^{-\tau\alpha}$ has the stationary point $\alpha_s = (\ln(K\tau))/\tau$, it is decreasing for all $\alpha < \alpha_s$ and increasing for all $\alpha > \alpha_s$, hence

$$B_1(K, \tau) = \{\alpha + i\pi/\tau : \alpha \in \mathbb{R},\ \alpha \geq K\} \qquad \text{for } K\tau \leq 1$$

and

$$B_1(K, \tau) = \{\alpha + i\pi/\tau : \alpha \in \mathbb{R},\ \alpha \geq (\ln(K\tau) + 1)/\tau\} \qquad \text{for } K\tau > 1.$$

Now, analysing the form of $B_2(K, \tau)$, where $\alpha = 0$, it can be obtained

$$B_2(K, \tau) = \{i\beta - Ke^{-i\tau\beta} : \beta \in \mathbb{R},\ 0 \leq \beta \leq \pi/\tau\}$$
$$= \{-K\cos(\tau\beta) + i(\beta + K\sin(\tau\beta)) : \beta \in \mathbb{R},\ 0 \leq \beta \leq \pi/\tau\}.$$

Equivalently, putting $\alpha = -K\cos(\tau\beta)$, then

$$B_2(K,\tau) = \left\{ \alpha + \mathrm{i}\left(\frac{\arccos(-\alpha/K)}{\tau} + \sqrt{K^2 - \alpha^2} \right) : \alpha \in \mathbb{R},\ -K \le \alpha \le K \right\}.$$

Notice that the function

$$f_2(\alpha) = \frac{\arccos(-\alpha/K)}{\tau} + \sqrt{K^2 - \alpha^2}, \qquad -K \le \alpha \le K$$

has the stationary point $\alpha_s = 1/\tau$, hence f_2 is increasing on its domain if $K\tau \le 1$ while it is increasing on $[-K, 1/\tau]$ and decreasing on $[1/\tau, K]$ if $K\tau > 1$. It remains to dispose with $B_3(K,\tau)$. Obviously,

$$B_3(K,\tau) = \{\alpha - Ke^{-\tau\alpha} : \alpha \in \mathbb{R},\ \alpha \ge 0\} = \{\alpha \in \mathbb{R} : \alpha \ge -K\}.$$

Thus, the border of $U_0^+(K,\tau)$, when (K,τ) is fixed is depicted in Figure 4.3.
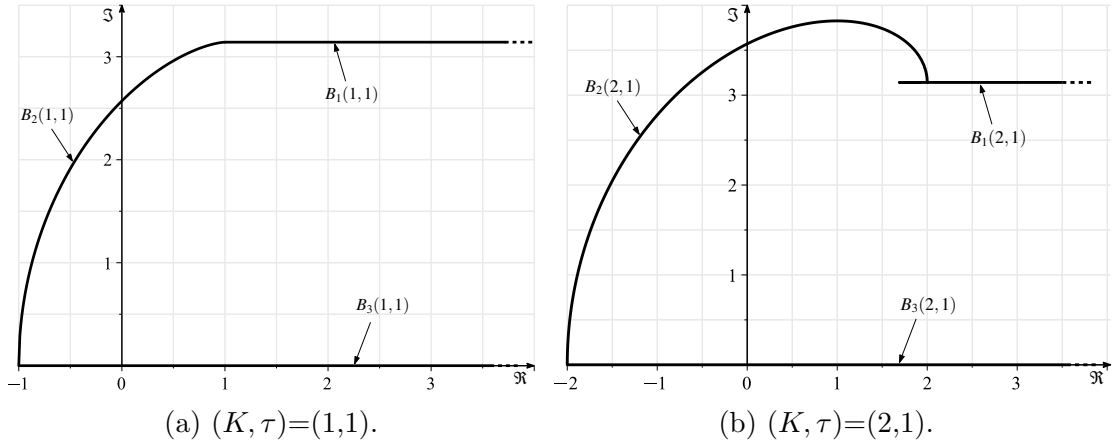

(a) $(K,\tau)=(1,1)$. (b) $(K,\tau)=(2,1)$.

Figure 4.3: Three border parts of the set $U_0^+(K,\tau)$.

Using appropriate shifties and symmetries described above one can obtain the set $U(K,\tau)$ of all $\lambda \in \mathbb{C}$ such that (4.17) admits a root with a positive or zero real part. This set is depicted on Figure 4.4.

Of course, the complement of $U(K,\tau)$ in the complex plane is the stability region $S(K,\tau)$, i.e. the set of all $\lambda \in \mathbb{C}$ such that (4.17) has all roots with negative real parts. We describe this set analytically. First let $\lambda \in \mathbb{C}$ be such that $-\pi < \tau\Im(\lambda) \le \pi$ and distinguish two cases with respect to the sign of K. For $K \in \mathbb{R}^+$, it holds $\lambda \in S(K,\tau)$ if and only if one of the following conditions is satisfied

(i) $\Re(\lambda) < -K$;
(ii) $\Re(\lambda) = -K$, $\Im(\lambda) \ne 0$;
(iii) $|\Re(\lambda)| \le K$, $|\Im(\lambda)| > f_2(\Re(\lambda))$.

Similarly, for $K \in \mathbb{R}^-$, it holds $\lambda \in S(K,\tau)$ if and only if one of the following conditions is satisfied

(i) $\Re(\lambda) < K$;
(ii) $\Re(\lambda) = K$, $\tau\Im(\lambda) \ne \pi$;
(iii) $|\Re(\lambda)| \le -K$, $\pi - |\Im(\lambda)| > f_2(\Re(\lambda))$.
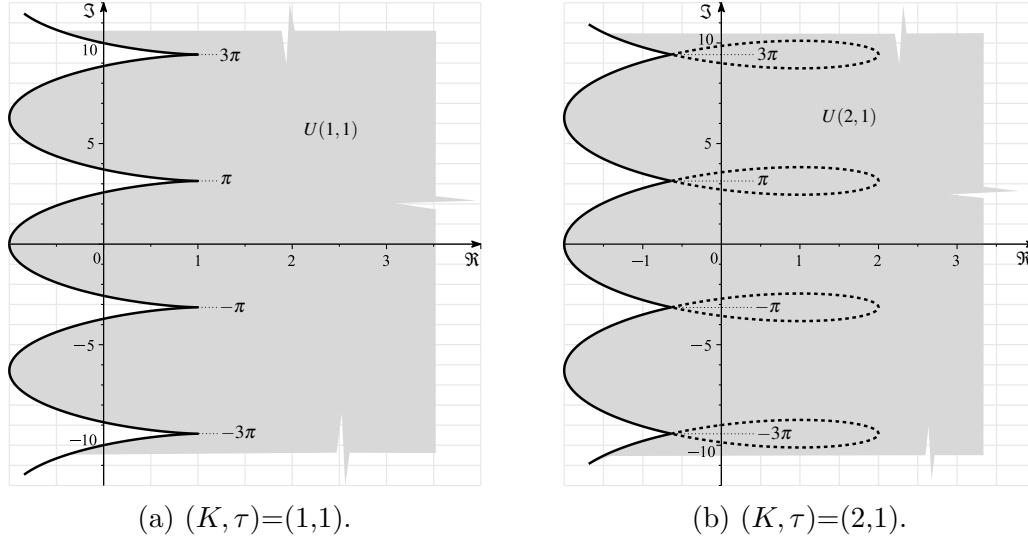
53

(a) (K,τ)=(1,1).

(b) (K,τ)=(2,1).

Figure 4.4: The instability set $U(K,\tau)$ in the complex plane.

Generalization of these conditions to a general complex λ is only a computational matter; in particular, it needs to employ periodic extensions of the functions $\tau|\Im(\lambda)|$ and $\pi - \tau|\Im(\lambda)|$ for $K \in \mathbb{R}^+$ and $K \in \mathbb{R}^-$, respectively. The required extension (and at the same time also unification of both sign cases for K) is provided by the function $\arccos[\operatorname{sgn}(K)\cos(\tau\Im(\lambda))]$. Thus, $\lambda \in S(K,\tau)$ if and only if any of the conditions of Theorem 12 (with λ_i replaced by λ) holds. $\qquad\square$

4.2.3 Stabilization of Unstable Focus (revised)

Now it can be shown, that Theorem 12 actually provides a generalization of the result presented in Section 4.2.1.

Recall, the system (4.5) has unstable focus in the origin. For easier manipulation it is convenient to rewrite the system into the form (4.16) used in Theorem 12, obtaining

$$\mathbf{x}'(t) = \begin{pmatrix} a - K & b \\ -b & a - K \end{pmatrix} \mathbf{x}(t) + KI\mathbf{x}(t - \tau), \tag{4.18}$$

where matrix B from (4.16) is in this case given by

$$B = \begin{pmatrix} a - K & b \\ -b & a - K \end{pmatrix}.$$

The eigenvalues λ_i of the matrix B can be computed from the characteristic equation

$$0 = \det \begin{pmatrix} a - K - \lambda & b \\ -b & a - K - \lambda \end{pmatrix}$$
$$\Rightarrow \lambda_{1,2} = (a - K) \pm \mathrm{i}b. \tag{4.19}$$

If the control is successful then the origin becomes asymptotically stable. Thus, according to the Theorem 12, one of the conditions (i)-(iii) must be satisfied for each λ_i given by (4.19). The next step is to analyse each condition and determine for which pairs $[K,\tau]$

the condition holds (if there are any). The following computation is given in more details as it will be later similarly applied for more complicated example.

(i) The case $\Re(\lambda_i) + |K| < 0$, λ_i given by (4.19)

$$(a - K) + |K| < 0 \Rightarrow \begin{cases} \text{if } K \geq 0 \text{ then } 0 > a \\ \text{if } K < 0 \text{ then } K > \frac{a}{2} . \end{cases}$$

Both results lead to $a < 0$ which is in contradiction with the assumption for unstable focus. This condition is not fulfilled.

(ii) The case $\Re(\lambda_i) + |K| = 0$, λ_i given by (4.19)

$$(a - K) + |K| = 0 \Rightarrow \begin{cases} \text{if } K \geq 0 \text{ then } 0 = a \\ \text{if } K < 0 \text{ then } K = \frac{a}{2} . \end{cases}$$

Similarly leads to $a \leq 0$ which is again in contradiction with the assumption.

(iii) The case $|\Re(\lambda_i)| - |K| < 0$, λ_i given by (4.19)

$$|a - K| - |K| < 0 \Rightarrow \begin{cases} a - K < -K & \text{for } K \in (-\infty, 0) \\ & \Rightarrow 0 > a \\ a - K < K & \text{for } K \in [0, a) \\ & \Rightarrow K > \frac{a}{2} \\ -(a - K) < K & \text{for } K \in [a, \infty) \\ & \Rightarrow 0 < a. \end{cases}$$

The case leading to $0 > a$ is not possible as it contradicts with the given task. The rest of the cases give the restriction for the control gain, namely

$$\frac{a}{2} < K.$$

Now, it is necessary to investigate for which time delays hold the second part of (iii), i.e. the condition for τ given by

$$\tau\sqrt{K^2 - (\Re(\lambda_i))^2} + \arccos\left(\frac{-\Re(\lambda_i)}{|K|}\right) < \arccos[\operatorname{sgn}(K)\cos(\tau\Im(\lambda_i))].$$

For $\lambda_1 = (a - K) + ib$, the inequality becomes

$$\tau\sqrt{K^2 - (a - K)^2} + \arccos\left(\frac{K - a}{|K|}\right) < \arccos[\operatorname{sgn}(K)\cos(\tau b)].$$

The case of $\lambda_2 = (a - K) - ib$ is not necessary to solve since imaginary part is present only in the term of cosine. Cosine is even function, i.e. $\cos(x) = \cos(-x)$, and therefore this case does not bring any new information. The previous computation gave the restriction for a and K which can be directly applied into the inequality. Since $K > 0$, there is no need for the absolute value and $\operatorname{sgn}(K) = 1$. Moreover,

condition $0 < \frac{a}{2} < K$ keeps the term under the root positive and the argument of arccosine is held in interval $[-1, 1]$ as desired. The inequality becomes

$$\tau\sqrt{a(2K - a)} + \arccos\left(\frac{K - a}{K}\right) < \arccos[\cos(\tau b)].$$

Now, the problem is, that τ is included in the term $\arccos[\cos(\tau b)]$. The function $\arccos(x)$ has domain of x equal to $[-1, 1]$ and range of values $[0, \pi]$. In this case, the argument of arccosine is given by cosine function and therefore it is convenient evaluate the term firstly for $\tau b \in (0, \pi]$ and $\tau b \in [-\pi, 0)$. The zero point is excluded because both τ and b are different from zero. Using the periodicity of cosine function, the domain can be extended for all $\tau b \in \mathbb{R} \setminus \{2n\pi\}$, where $n \in \mathbb{Z}$. It is useful to add that the negative values of τb are accomplished only by taking $b < 0$ since $\tau \in \mathbb{R}^+$.

(a) If $\tau b \in (0, \pi]$ then $\arccos[\cos(\tau b)] = \tau b$. Thus,

$$\tau\sqrt{a(2K - a)} + \arccos\left(\frac{K - a}{K}\right) < \tau b$$

$$\Rightarrow \tau > \frac{\arccos\left(\frac{K - a}{K}\right)}{b - \sqrt{a(2K - a)}}. \qquad (4.20)$$

(b) If $\tau b \in [-\pi, 0)$ then $\arccos[\cos(\tau b)] = -\tau b$. Thus,

$$\tau\sqrt{a(2k - a)} + \arccos\left(\frac{K - a}{K}\right) < -\tau b$$

$$\Rightarrow \tau < \frac{-\arccos\left(\frac{K - a}{K}\right)}{b + \sqrt{a(2K - a)}}. \qquad (4.21)$$

In the last step, the periodicity of cosine must be taken into consideration. Since cosine has period equal to 2π the conditions on τb can be extended from (4.20) and (4.21) by taking intervals $(0, \pi] + 2n\pi$ and $[-\pi, 0) + 2n\pi$, where $n \in \mathbb{Z}$ respectively. Then new restrictions for τ are given by

(a) If $\tau b \in (0, \pi] + 2n\pi$ then $\arccos[\cos(\tau b)] = \tau b - 2n\pi$. For $n = 0, 1, 2, \ldots$ the time delay

$$\tau > \frac{2n\pi + \arccos\left(\frac{K - a}{K}\right)}{b - \sqrt{a(2k - a)}}. \qquad (4.22)$$

(b) If $\tau b \in [\pi, 2\pi) + 2n\pi$ then $\arccos[\cos(\tau b)] = -\tau b + 2(n + 1)\pi$. For $n = 0, 1, 2, \ldots$ the time delay

$$\tau < \frac{(2n + 1)\pi - \arccos\left(\frac{K - a}{K}\right)}{b + \sqrt{a(2K - a)}}. \qquad (4.23)$$

Taking the threshold of (4.22) as $\tau^+ = \frac{2n\pi + \arccos\left(\frac{K-a}{K}\right)}{b - \sqrt{a(2k-a)}}$ and threshold of (4.2.3) as $\tau^- = \frac{(2n+1)\pi - \arccos\left(\frac{K-a}{K}\right)}{b + \sqrt{a(2K-a)}}$, the final condition for time delay can be written as

$$\tau^+ < \tau < \tau^- \quad \text{for } n = 0, 1, 2, \ldots. \qquad (4.24)$$

56

The results obtained by this method are following. In the case of unstable focus given by (4.5) and control scheme (4.18), the condition (iii) holds for both eigenvalues of (4.19), if the control parameters are chosen from the region restricted by $K > \frac{a}{2}$ and τ satisfies $\tau^+ < \tau < \tau^-$, where τ^+, τ^- are given by (4.22), (4.2.3), respectively. In the comparison to the results obtained earlier by (4.2.3), it is easy to see that this approach leads to the same domain of control as in the case of control introduced by Hövel in [27].

Another comparison can be done for a case of a saddle point in 2D which was also studied by Hövel. This case will not be presented here, however, it is easy to prove, that none of the condition (i)-(iii) given by the Theorem 12 can be satisfied for any pair $[K, \tau]$ due to the real positive eigenvalue of a saddle point.

Finally, it can be added that stability conditions of Theorem 12 can be applied to a more general stabilization problem than studied in [27].

4.2.4 Stabilization of chaotic Rössler system

In the following part, Theorem 12 will be applied to a particular Rössler system and numerical experiments will be included to support the theoretical results. Firstly, the parameters of the system are chosen according to the previous analysis of Rössler system given in Chapter 3. It was observed, that for the choice $a = b = 0.1$ and $c = 14$ the system is chaotic. The procedure of applying the stability theorem is similar to the case of unstable focus, however, it is convenient to rewrite the condition (i)-(iii) in the following way.

Remark 13. *Conditions* (i)-(iii) *of Theorem 12, where* $B = Df(\mathbf{x}^*) - KI$ *is the linearised matrix of controlled system* (4.16)*, can be equivalently rewritten as*

(i') $\Re(\hat{\lambda}_i) - K + |K| < 0$ *and* τ *is arbitrary;*

(ii') $\Re(\hat{\lambda}_i) - K + |K| = 0$, $K \neq 0$ *and* $\tau\Im(\hat{\lambda}_i) - \arg(K) \neq 2\ell\pi$ *for any* $\ell \in \mathbb{Z}$;

(iii') $|\Re(\hat{\lambda}_i) - K| - |K| < 0$

and $\tau\sqrt{K^2 - (\Re(\hat{\lambda}_i) - K)^2} + \arccos\left(\frac{-\Re(\hat{\lambda}_i) + K}{|K|}\right) < \arccos[\mathrm{sgn}(K)\cos(\tau\Im(\hat{\lambda}_i))]\,,$

where $\hat{\lambda}_i, = 1, \ldots, n$ *are eigenvalues of* $A = Df(\mathbf{x}^*)$*, i.e. the Jacobian matrix evaluated at* $\mathbf{x}^*$*. Equivalently, the fixed point* $\mathbf{x}^*$ *is stabilized if any of the conditions is satisfied for each eigenvalue* $\hat{\lambda}_i$ *of* A*.*

As an application of Theorem 12 the Rössler system with parameters $a = b = 0.1$ and $c = 14$ given by the system of equations

$$\begin{aligned}
x' &= -y - z \\
y' &= x + 0.1y \\
z' &= 0.1 + z(x - 14),
\end{aligned} \tag{4.25}$$

is investigated. For this particular system there exist two unstable equilibria

$$\mathbf{x}_1^* = [13.9993, \, -139.9929, \, 139.9929]\,,$$
$$\mathbf{x}_2^* = \left[7.1432 \cdot 10^{-4}, \, -7.1432 \cdot 10^{-3}, \, 7.1432 \cdot 10^{-3}\right]$$

with corresponding eigenvalues

$$\lambda_r^1, \approx 0.099286 \qquad \lambda_{+/-}^1 \approx -2.5149160 \cdot 10^{-8} \pm 11.874038\,\mathrm{i}\,,$$
$$\lambda_r^2, \approx -13.998778 \qquad \lambda_{+/-}^2 \approx 0.049746 \pm 0.998755\,\mathrm{i}\,.$$

At this point, similar analysis to the case of unstable focus is necessary. For the equilibrium point $\mathbf{x}_1^*$, it can be directly computed that the domain of control is empty due to the positive real eigenvalue. On the other hand, investigation of the conditions (i')-(iii') for $\mathbf{x}_2^*$ yields the following results.

The case λ_r^2: The eigenvalue is real valued (negative), hence $\Re(\lambda_r^2) = \lambda_r^2$. Since λ_r^2 has to satisfy one of the condition (i')-(iii'), for any pair $[K, \tau]$ must hold either

$$\frac{\lambda_r^2}{2} \leq K, \quad \tau \in \mathbb{R}^+ \quad \text{or} \quad K < \frac{\lambda_r^2}{2}, \quad \tau < \frac{\pi - \arccos\left(\frac{\lambda_r^2 - K}{K}\right)}{\sqrt{\lambda_r^2(2K - \lambda_r^2)}}$$

The case $\lambda_{+/-}^2$: The eigenvalues are complex with positive real part. Hence, it is again sufficient to run the computation only for one of the them. Choosing λ_+^2, it can be easily seen that only condition (iii') satisfies, namely if $K > \frac{\Re(\lambda_+^2)}{2}$ (> 0). Condition for the time delay is then given

$$\frac{2n\pi + \arccos\left(\frac{K - \Re(\lambda_+^2)}{K}\right)}{\Im(\lambda_+^2) - \sqrt{\Re(\lambda_+^2)(2K - \Re(\lambda_+^2))}} < \tau < \frac{(2n+1)\pi - \arccos\left(\frac{K - \Re(\lambda_+^2)}{K}\right)}{\Im(\lambda_+^2) + \sqrt{\Re(\lambda_+^2)(2K - \Re(\lambda_+^2))}}, \quad (4.26)$$

where $n = 0, 1, 2, \ldots$. This is similar to the result obtained in case of unstable focus.

According to the results (4.26) obtained by using Theorem 12, the domain of control parameters that can be used to stabilize the Rössler system (4.25) is depicted in Figure 4.5 for $n = \{0, 1, 2, 3\}$.
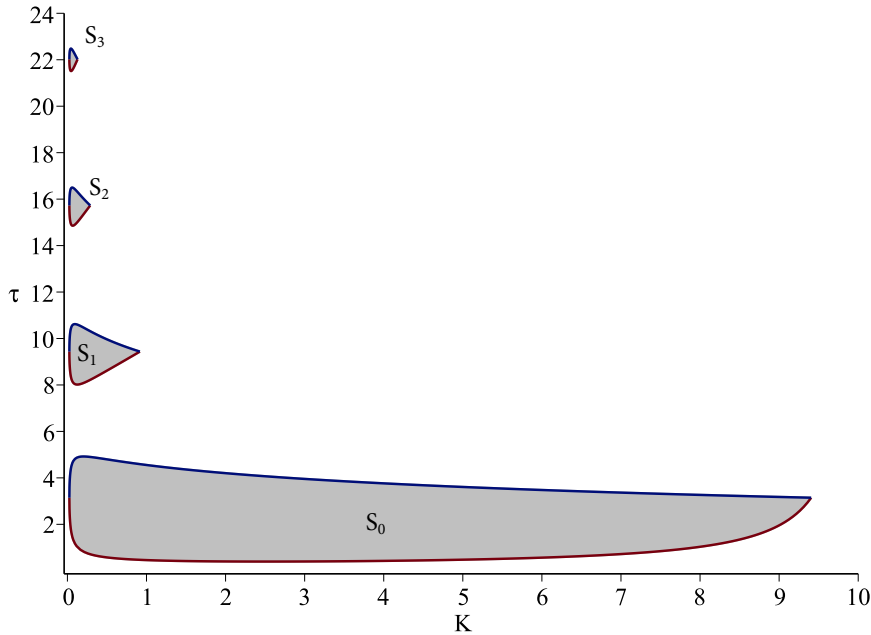

Figure 4.5: Domain of control in (K,τ)-plane.

Numerical experiments

To verify the theoretical results obtained above, few pairs $[K, \tau]$ will be tested numerically using the implemented function in Matlab called dde23. [28] The function dde23 solves

the initial value problem for a system of delay differential equations (DDEs) with constant time delays. The method is closely related to ordinary differential equations solver ode23 based on the explicit Runge–Kutta methods.

The main difference between ODEs and DDEs consists in the initial data. While the solution of an ODE is determined by its value at the initial point $t = t_0$, in the case of DDEs it is necessary to prescribe the solution of the problem also for times preceding the initial one. Thus, not only the value of the solution at the initial point, but also the 'history' must be provided. If τ is the time delay (or the largest among the delays), then on the interval $t_0 - \tau < t < t_0$, it is necessary to define the solution of $\mathbf{x}(t - \tau)$ since $t - \tau$ refers to a time before the initial point.

In the case of dde23, the history data are usually given by a constant function. This approximation causes a problem of discontinuities of low-order derivatives. Thus, the solution close to the initial point can be rough. However, the goal of the method is to determine the behaviour of the system as $t \to \infty$ and therefore the early difficulties can be ignored.

The method dde23 was used to prove that choosing a pair of control parameters $[K, \tau]$ from the domain of control given by (4.26) and depicted in Figure 4.5 will lead to stabilization of the fixed point $\mathbf{x}_2^*$. For several examples the history data was chosen uniformly $H = [-1, -1, 0.1]$ and $[K, \tau]$ was taken from the subsets S_0 and S_1.

(a) $[K, \tau] = [1.5, 0.5]$.

(b) $[K, \tau] = [2.5, 1.5]$.
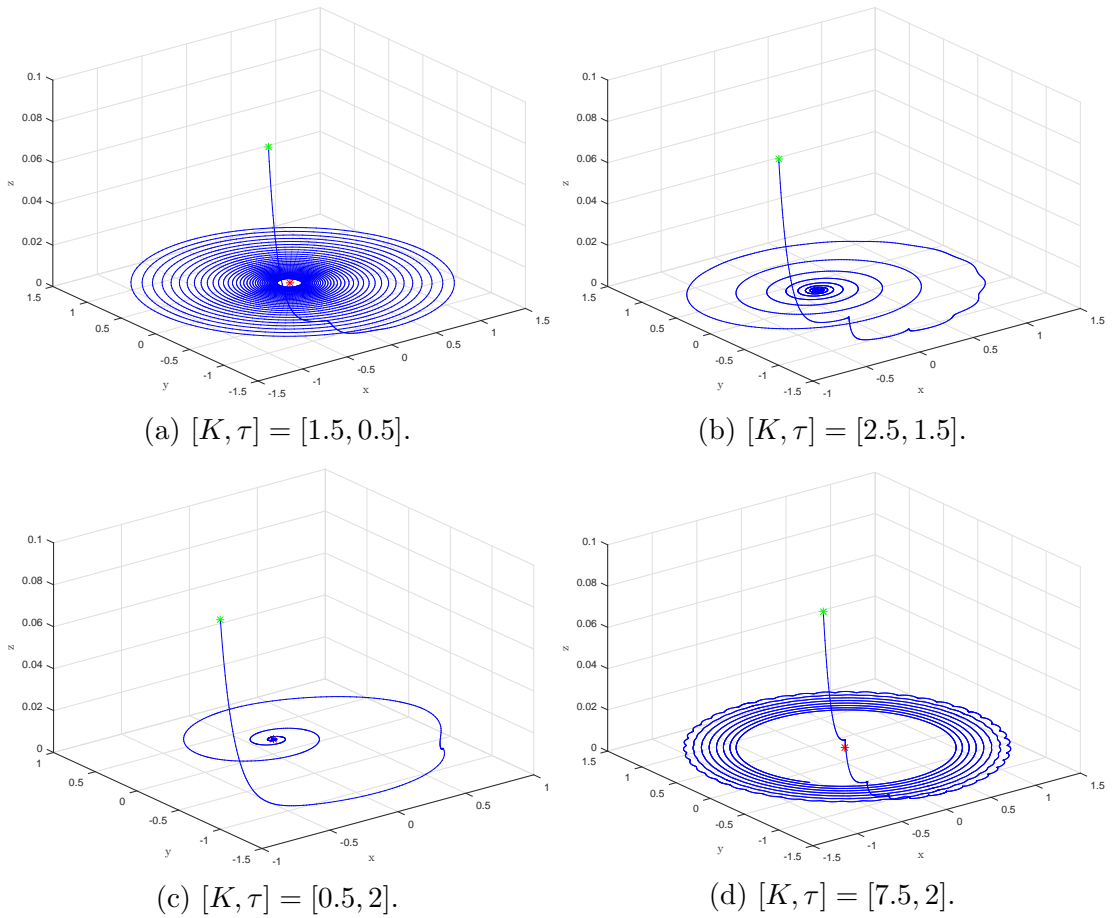
(c) $[K, \tau] = [0.5, 2]$.

(d) $[K, \tau] = [7.5, 2]$.

Figure 4.6: Stabilization of $\mathbf{x}_2^*$ for suitable pairs $[K, \tau] \in S_0$.

In Figure 4.6, four pairs of $[K, \tau]$ were chosen from the set S_0. It is easy to see, that the choice presented in Figure 4.6c is the most efficient as the trajectory moves fast towards the equilibrium point. On the other hand, under the choice $[K, \tau] = [7.5, 2]$ depicted in Figure 4.6d the trajectory is moving slowly towards the equilibrium point.

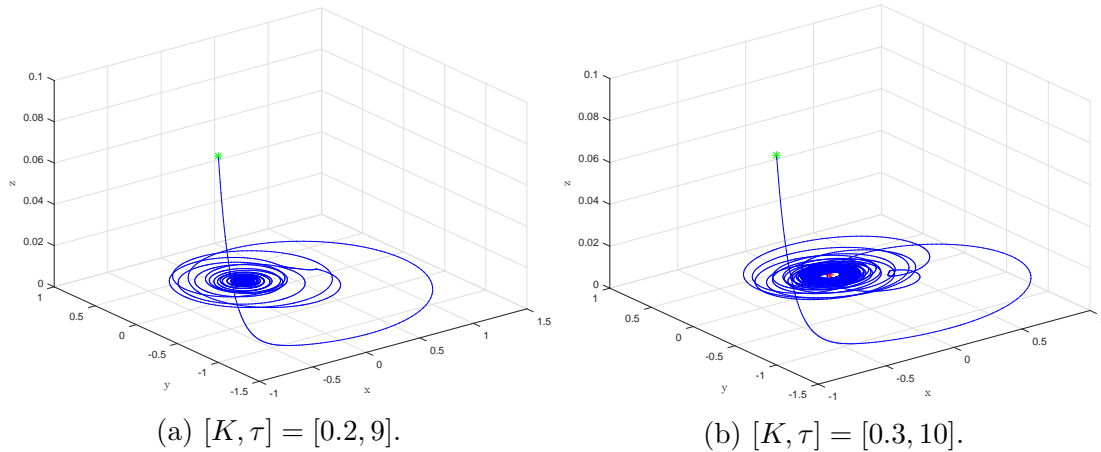Similarly, pairs from region S_1 are investigated and plotted in Figure 4.7.

(a) $[K, \tau] = [0.2, 9]$.

(b) $[K, \tau] = [0.3, 10]$.

Figure 4.7: Stabilization of $\mathbf{x}_2^*$ for suitable pairs $[K, \tau] \in S_1$.

In the last examples the influence of the chosen history data was tested. It was observed, that the value of the history data can be chosen freely as illustrate the choices depicted in Figure 4.8.
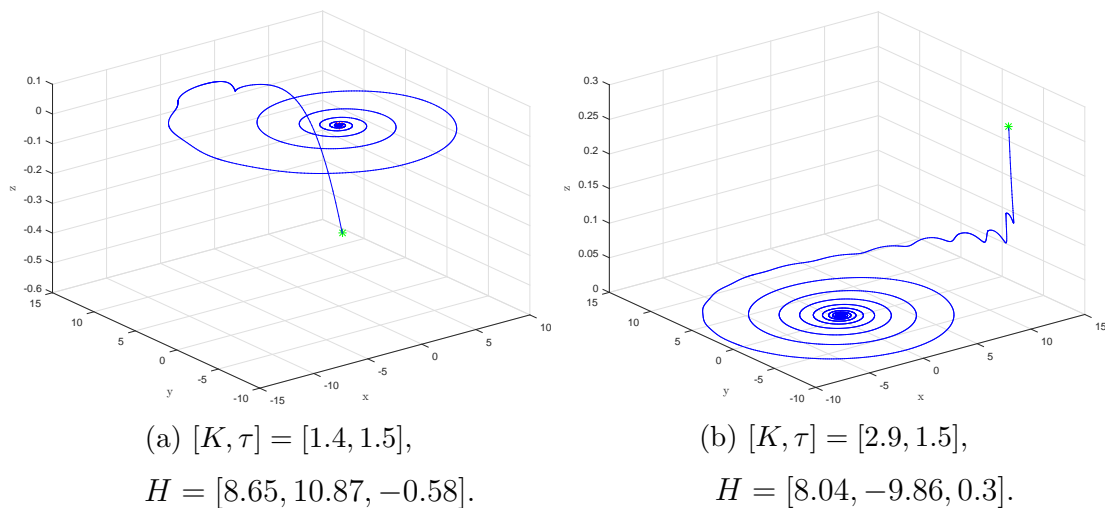

(a) $[K, \tau] = [1.4, 1.5]$,

$H = [8.65, 10.87, -0.58]$.

(b) $[K, \tau] = [2.9, 1.5]$,

$H = [8.04, -9.86, 0.3]$.

Figure 4.8: Stabilization of $\mathbf{x}_2^*$ for suitable pairs $[K, \tau]$ using different history.

5 SYNCHRONIZATION OF CHAOTIC SYSTEMS

As it was already mentioned and shown in the previous parts of this work, the sensitivity on the initial conditions plays a significant role in the chaos theory. Therefore, the evolution of chaotic system in time will differ even for two very close starting points, since the trajectories separate exponentially in time. Yet, the trajectories remain trapped inside the strange attractor. In the previous chapter, the concept of controlling chaos was presented together with some examples of stabilization unstable equilibrium points. It was proven, that for certain conditions, all trajectories starting at a point from the basin of attraction will eventually reach the desired state, in this case the equilibrium point.

Another way, how to think about control of dynamical systems, is the idea of synchronization. In the original meaning, synchronization is understood as an agreement in time of different processes. In the theory of chaos, synchronization refers to a process, when two (or more) chaotic systems (not necessarily identical) are forced to adapt their behaviour to a common property. According to the recent studies, the common property can be defined by the desired stage of synchronization. The strongest request, i.e. complete unification of the states of the systems, is connected to the method called complete synchronization. This method can be applied in the case of two identical systems starting at different initial points. The process of synchronization is then successful, if the trajectories of both systems converge to the same values and remain in step with each other. This approach will be further discussed in this chapter, and applied in examples for synchronizing two identical Rössler systems.

Other approaches do not require the trajectories to merge completely, but specify the nature of the desired synchrony. Therefore, they are also more suitable for cases of nonidentical systems. The phase synchronization is based on a weak coupling of two systems. During the process, the phases become locked on some value and provide the trajectories to be in phase with each other, while the amplitudes may remain completely diverse. In case of lag synchronization, on the other hand, the states of the two systems become nearly identical due to a stronger coupling, however, shifted in time. Thus, if s_1, s_2 are states of the two systems, the lag synchronization is reached if $s_1(t) \approx s_2(t - \tau)$. The stronger the coupling scheme, the smaller the time lag τ. At the strongest schemes, τ can almost approach zero, providing almost complete synchronization.

The method of generalized synchronization extends the case of complete synchronization to a problem of nonidentical systems. If $\mathbf{x}$, $\mathbf{y}$ are trajectories of two different systems, then probably, there does not exist a coupling scheme which could provide an equality between the synchronized states. Therefore, the method defines a relation $h : \mathbf{y} = h(\mathbf{x})$, according to that each state of one system is completely determined by the state of the other system. The method can be applied as well to two identical systems, moreover, if $h(\mathbf{x})$ is an identity, then generalized synchronization becomes equivalent to complete synchronization. An extended overview of the methods can be found in [29].

The common property of the methods described above is that after the time needed for synchronization, the systems remain in synchrony. However, there exist several methods which cannot secure synchrony for all time, since local bursts occur. An example exhibiting this phenomena is the imperfect phase synchronization or the intermittent lag synchronization. All methods can be further divided according to the use of specific coupling scheme. Two basic concepts will be described for the case of the complete synchronization method, however, they do not differ in principal for the rest of the methods.

Finally, for each method there is necessity of restrictions for successful synchronization. Usually, they are given as a restriction on the Lyapunov exponents spectrum which was introduced in the first chapter.

5.1 Methods of complete synchronization

Complete (identical) synchronization is based on coupling two identical systems (with same parameters) and synchronization of their trajectories onto one common trajectory. However, it is necessary to distinguish the way how the systems influence each other during the process. If one of the system remains unaltered during the process of synchronization, the concept is called unidirectional coupling or drive-response coupling. This type of coupling is widely used for secure communication by using chaotic signals. On the other hand, if both of the systems are changed and influenced by each other during the process, the concept is called bidirectional coupling. This type can be applied in the physiology, e.g. while synchronizing the cardiac and respiratory system.

As this work follows up mainly continuous systems, the following methods will be described also only for continuous cases. However, the ideas can be applied as well for discrete cases.

5.1.1 Drive-Response configuration

This method, also called master-slave configuration or unidirectional coupling, is based on forming a global system out of two subsystems, where one of them evolves freely and drives the evolution of the other. As a result, the response system is forced to forget its initial data and follow the evolution of the master. The method can be further divided according to the coupling scheme.

Pecora and Caroll

One of the first works investigating the possibility of synchronization of two identical chaotic systems was given by L. Pecora and T. Caroll. [11], [30] Their method is based on the master-slave configuration. Suppose a chaotic dynamical system $\mathbf{x}' = f(\mathbf{x})$ in $\mathbb{R}^n$ which can be decomposed into two subsystems

$$\mathbf{v}' = g(\mathbf{v}, \mathbf{w}),$$
$$\mathbf{w}' = h(\mathbf{v}, \mathbf{w}),$$

where $\mathbf{x} = (\mathbf{v}, \mathbf{w})$, $\mathbf{v} = (x_1, \ldots, x_m)$, $g = (f_1(\mathbf{x}), \ldots, f_m(\mathbf{x}))$, $\mathbf{w} = (x_{m+1}, \ldots, x_n)$ and $h = (f_{m+1}(\mathbf{x}), \ldots, f_n(\mathbf{x}))$. Now create a new subsystem $\hat{\mathbf{w}}$ identical to $\mathbf{w}$. The new system of interest is then given by

$$\mathbf{v}' = g(\mathbf{v}, \mathbf{w}), \qquad \mathbf{w}' = h(\mathbf{v}, \mathbf{w}), \qquad \hat{\mathbf{w}}' = h(\mathbf{v}, \hat{\mathbf{w}}).$$

The original two subsystems $\mathbf{v}$, $\mathbf{w}$ refer to the driving subsystem, while the $\hat{\mathbf{w}}$ corresponds to the response subsystem. Particularly in this case, the expression 'v-drive configuration' is often used. The subsystems are in synchrony if the trajectories of the driving system $\mathbf{w}$ and its replica $\hat{\mathbf{w}}$ under the same driving signal $\mathbf{v}$ are equal. Let $\Delta \mathbf{w} = \hat{\mathbf{w}} - \mathbf{w}$. The subsystems can be synchronized only if $\Delta \mathbf{w} \to 0$ as $t \to \infty$. The necessary condition for

successful synchronization is based on the sign of the Lyapunov exponents of the response system which are called conditional. All conditional Lyapunov exponents must be negative, otherwise the synchronized state would not be stable. Thus, for many systems, only some equations are suitable to be applied as the drive.

Active-passive decomposition method

The method introduced by Pecora and Caroll is specific considering the suitable form of driving signal. The active-passive decomposition represents more general approach, where the driving signal can be chosen more freely if certain conditions hold. [31] The method is based on formal rewriting of the autonomous dynamical system as a nonautonomous one

$$\mathbf{x}' = f(\mathbf{x}, s(t)), \tag{5.1}$$

where $s(t)$ corresponds to the driving signal given as $s(t) = h(\mathbf{x})$ or $s' = h(\mathbf{x}, s)$. Then, the same driving signal is applied on the identical system which can be rewritten as

$$\mathbf{y}' = f(\mathbf{y}, s(t)).$$

Let $\mathbf{e} = \mathbf{x} - \mathbf{y}$ be the difference between the two states. If the differential equation

$$\mathbf{e}' = \mathbf{x}' - \mathbf{y}' = f(\mathbf{x}, s) - f(\mathbf{y}, s) \tag{5.2}$$

has a stable fixed point at $\mathbf{e} = \mathbf{0}$, then the synchronization is successful, i.e. $\mathbf{x} = \mathbf{y}$. The stability of (5.2) at $\mathbf{e} = \mathbf{0}$ can be determined by using Lyapunov function. Nevertheless, as in the previous case, the condition on the negative conditional Lyapunov exponents of the system (5.1) must be satisfied.

Negative feedback control

Synchronization by negative feedback control is very similar to the processes discussed in the previous chapter. Consider two identical chaotic systems $\mathbf{x}' = f(\mathbf{x})$ and $\mathbf{y}' = f(\mathbf{y})$. The systems are coupled unidirectionally in the way that the difference between two corresponding variables is applied to the appropriate equation of the driven system as a negative feedback. Together with a suitable value of the feedback gain K, the term of the control signal has the form

$$F(t) = K(x_i(t) - y_i(t)). \tag{5.3}$$

To achieve the synchrony between the two systems, the control gain K ($K > 0$) must be chosen in the way that the number of positive Lyapunov exponents of the new composed system and the driving system must be the same. For chaotic system in 3D it means, that the composed system is allowed to have exactly one positive Lyapunov exponent.

Generally, the control signal can be added to more than just one equation of the driven system, which will enlarge the region of suitable control gains for successful synchronization. Moreover, this method is non-invasive since the control disappears when the two systems synchronize onto one trajectory.

5.1.2 Bidirectional coupling

In contrast to the master-slave methods, the bidirectional coupling is based on interaction between the systems which is achieved by adding a term of additional dissipation into both systems

$$\begin{aligned}
\mathbf{x}' &= f(\mathbf{x}) + D(\mathbf{y} - \mathbf{x}) \\
\mathbf{y}' &= f(\mathbf{y}) + D(\mathbf{x} - \mathbf{y}).
\end{aligned} \tag{5.4}$$

If the matrix presenting the dissipation has a particular form $D = d\,I$ then the synchrony is achieved for $d > \frac{1}{2}\Lambda_{max}$, where Λ_{max} is the largest Lyapunov exponent of unsynchronized system.

5.2 Synchronization of two Rössler systems

In this part of the chapter, some of the methods mentioned above will be tested on Rössler system, which is the main subject of this work. The choice of parameters remains unchanged, i.e. $a = b = 0.1$ and c is chosen specifically for each method.

Negative feedback control

The synchronization by negative feedback is possible only for certain control gains and driving signals. Thus, the task is to find the suitable configurations which will fulfil the condition of number of Lyapunov exponents. Firstly, the parameter c is chosen to be $c = 18$, which corresponds to the chaotic behaviour and the control signal is of the form given in (5.3).

The method will be demonstrated with control by variable x and with control by variables x and y. Analysis for control by variable y, z and their combinations could be done similarly.

- Control by variable x: The configuration

$$\begin{aligned}
x' &= -y - z\,, & \hat{x}' &= -\hat{y} - \hat{z} + K(x - \hat{x})\,, \\
y' &= x + 0.1y\,, & \hat{y}' &= -\hat{x} + 0.1\hat{y}\,, \\
z' &= 0.1 + z(x - 18)\,, & \hat{z}' &= 0.1 + \hat{z}(\hat{x} - 18)
\end{aligned}$$

  was tested for several values of K for which the number of positive Lyapunov exponents is the same in composed system and in the original driving system. Results for $K = 0.8$, 2.5 can be seen in Figures 5.1 and 5.2. Each figure shows the evolution in variables x, $\hat{x}$, y and $\hat{y}$ and the difference between the corresponding ones. For $K = 0.2$ (see Figure 5.3), on the other hand, it is not possible to reach the synchrony.

- Control by two variables (x and y): The configuration

$$\begin{aligned}
x' &= -y - z\,, & \hat{x}' &= -\hat{y} - \hat{z} + K(x - \hat{x})\,, \\
y' &= x + 0.1y\,, & \hat{y}' &= -\hat{x} + 0.1\hat{y} + K(y - \hat{y})\,, \\
z' &= 0.1 + z(x - 18)\,, & \hat{z}' &= 0.1 + \hat{z}(\hat{x} - 18)
\end{aligned}$$

  was tested for $K = 0.2$ to prove that the control by two variables can enlarge the region of suitable control gains. For this configuration the driven system merged with its master as can be seen in Figure 5.4.
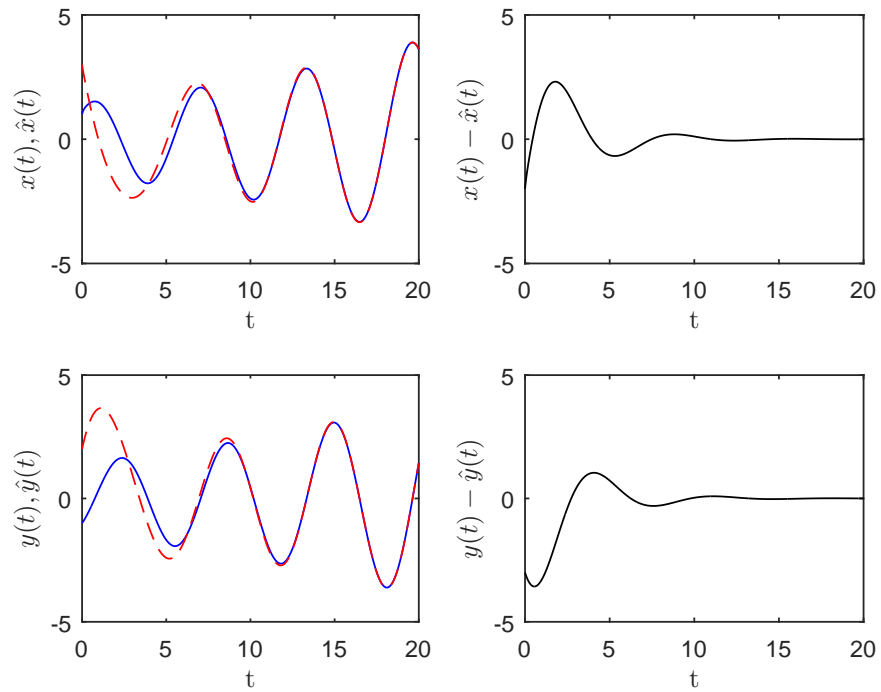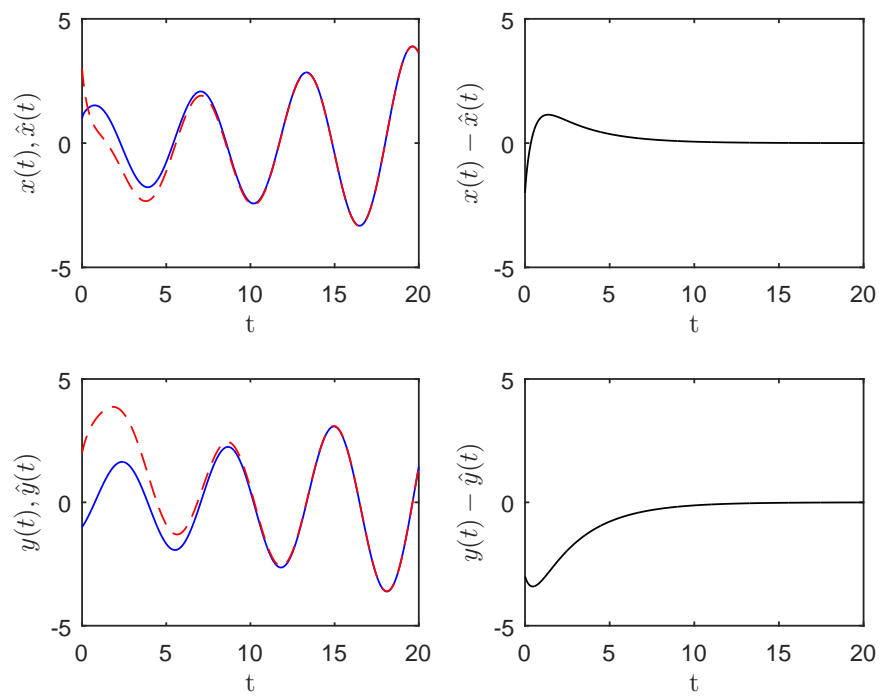
Figure 5.1: Control by variable x, $K = 0.8$.
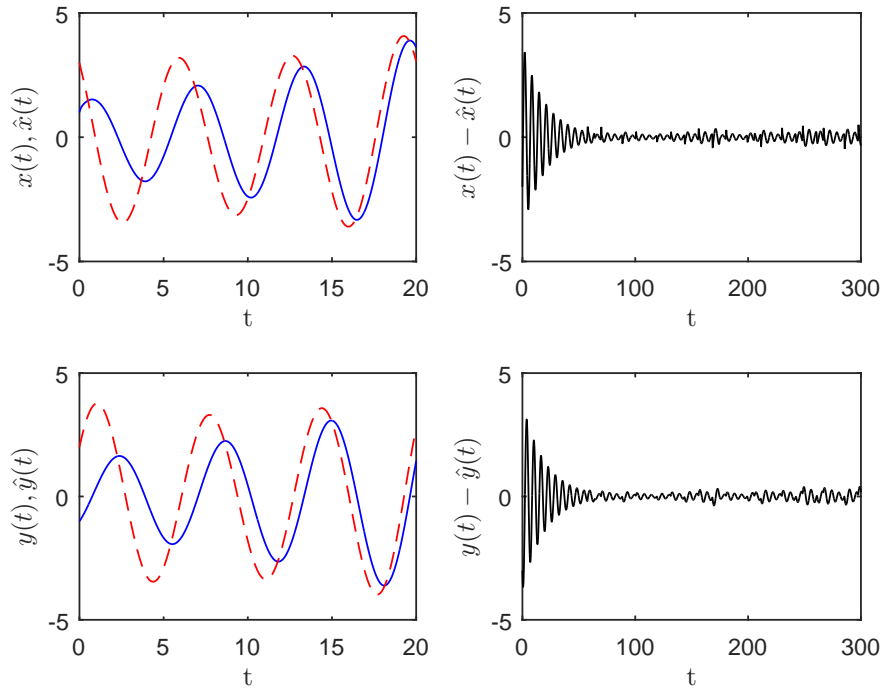

Figure 5.2: Control by variable x, $K = 2.5$.

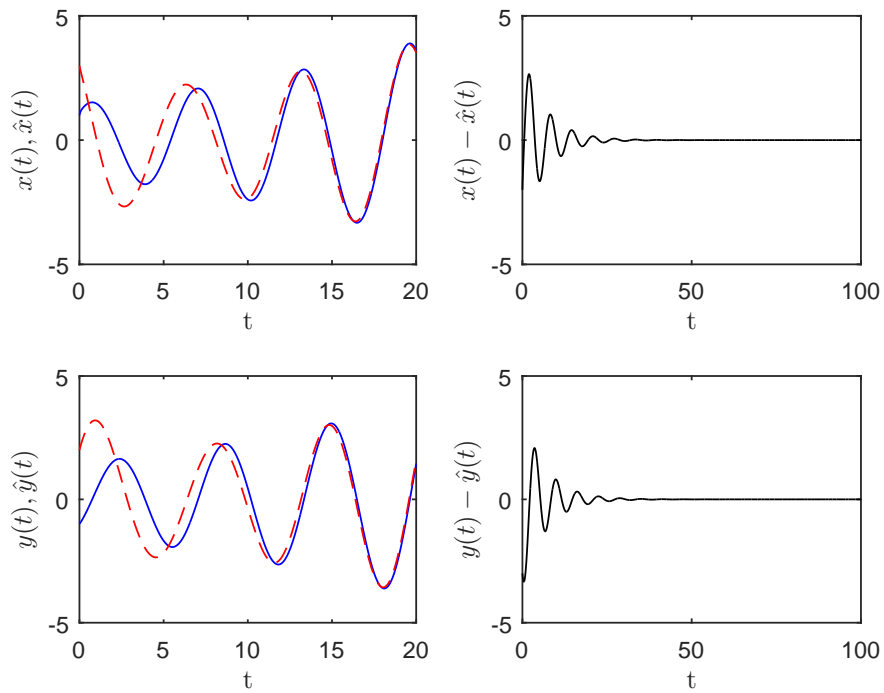Figure 5.3: Unsuccessful synchronization; control by variable x, $K = 0.2$.

Figure 5.4: Successful synchronization; control by variables x and y, $K = 0.2$.

Bidirectional coupling

The bidirectional coupling method given by (5.4) was tested on Rössler system with parameter $c = 14$. The dissipative term was taken as $D = d\,I$. For the original system, the largest Lyapunov exponent is approximately $\Lambda_{max} \approx 0.1$. Thus, taking any $d > 0.05$ should lead to success. The coupled system has the form

$$
\begin{aligned}
x' &= -y - z + d(\hat{x} - x) & \hat{x}' &= -\hat{y} - \hat{z} + d(x - \hat{x}) \\
y' &= x + 0.1y + d(\hat{y} - y) & \hat{y}' &= -\hat{x} + 0.1\hat{y} + d(y - \hat{y}) \\
z' &= 0.1 + z(x - 14) + d(\hat{z} - z) & \hat{z}' &= 0.1 + \hat{z}(\hat{x} - 14) + d(z - \hat{z}).
\end{aligned}
\tag{5.5}
$$

Some of the particular choices of d are presented in Figures 5.5-5.9. Again, each figure shows the evolution in variables x, $\hat{x}$, y and $\hat{y}$ and the difference between the corresponding ones. For $d = 0.06, 0.1, 2.5, 12$ the synchrony is easy to see, since the differences between the variables approach zero after some time. From the calculations also yield, that with increasing d the convergence to zero is faster. On the other hand, for $d = 0.03$ (which is less than $\frac{1}{2}\Lambda_{max}$) the synchronization is not successful as it was expected (see Figure 5.9).
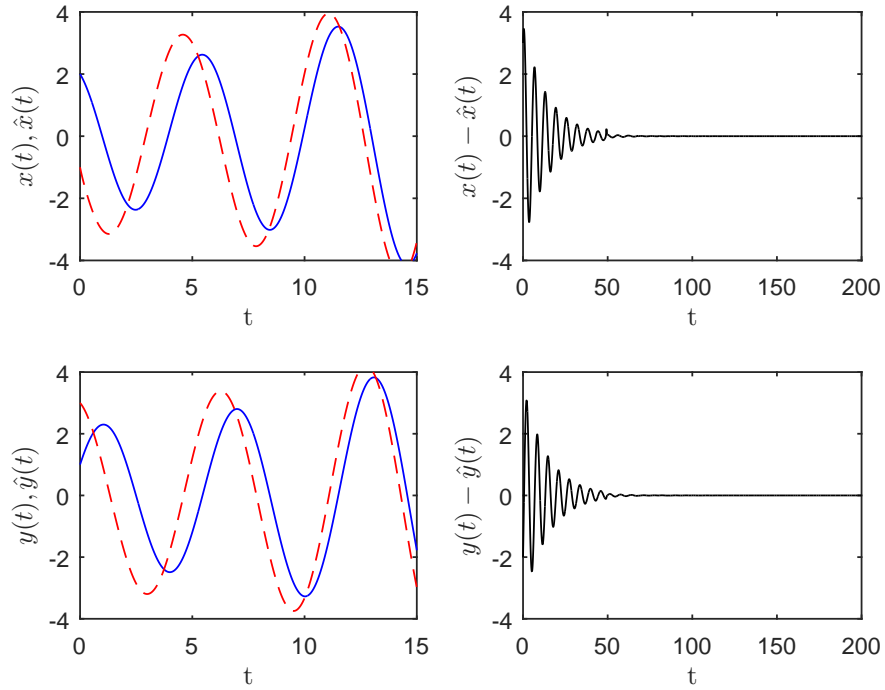

Figure 5.5: Bidirectional coupling, $d = 0.06$.
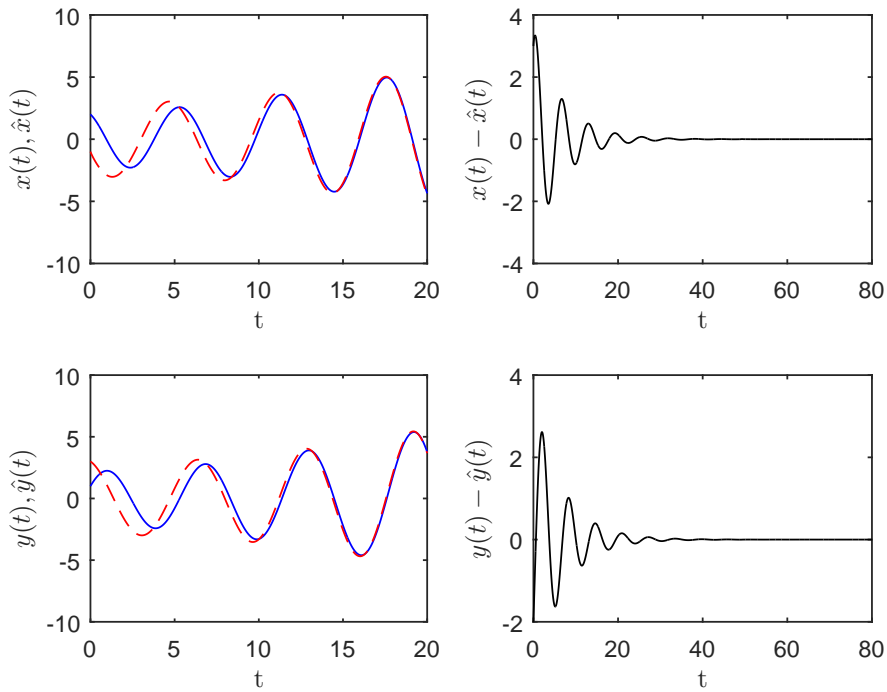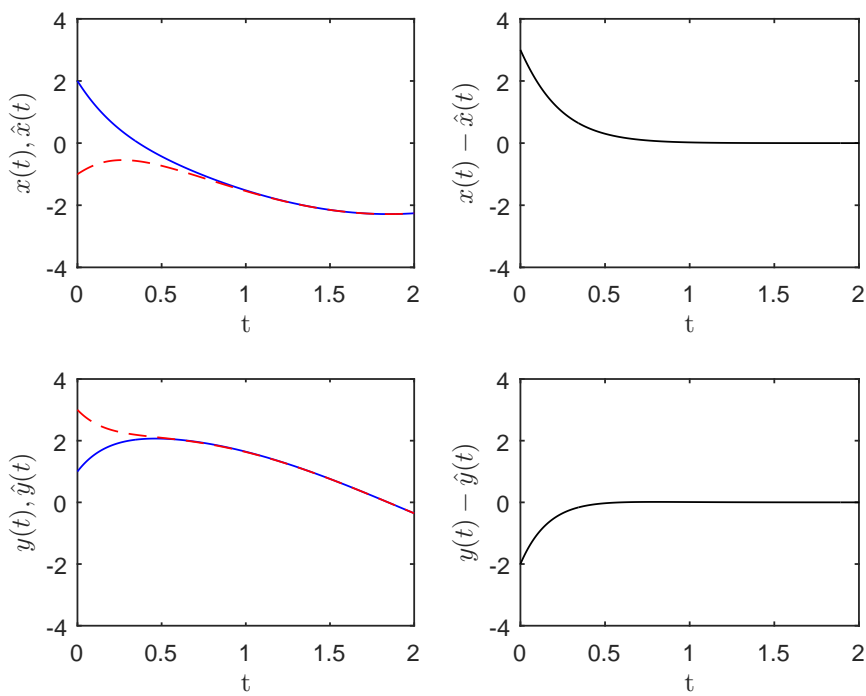
Figure 5.6: Bidirectional coupling, $d = 0.1$.

Figure 5.7: Bidirectional coupling, $d = 2.5$.

68
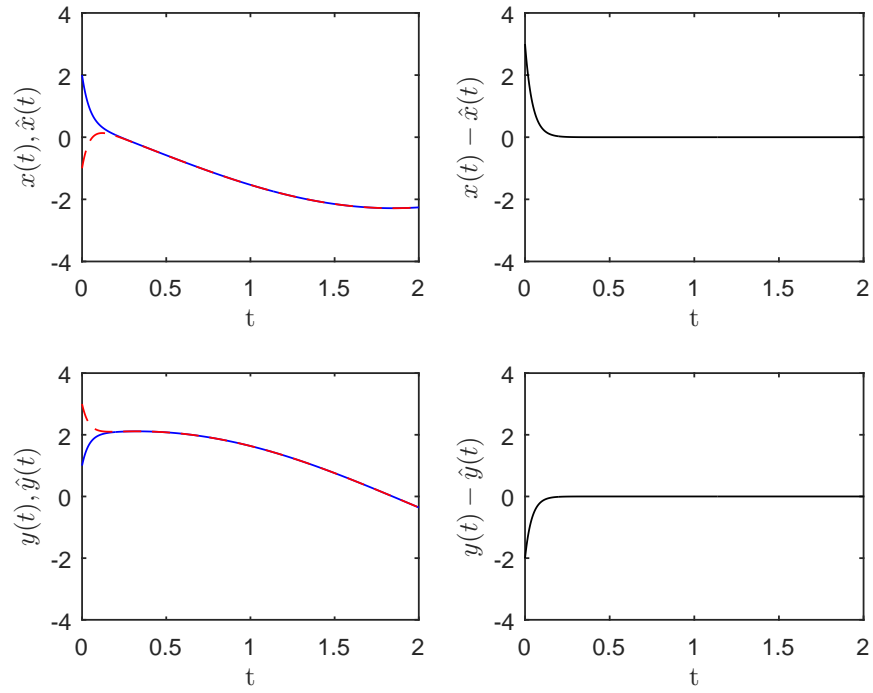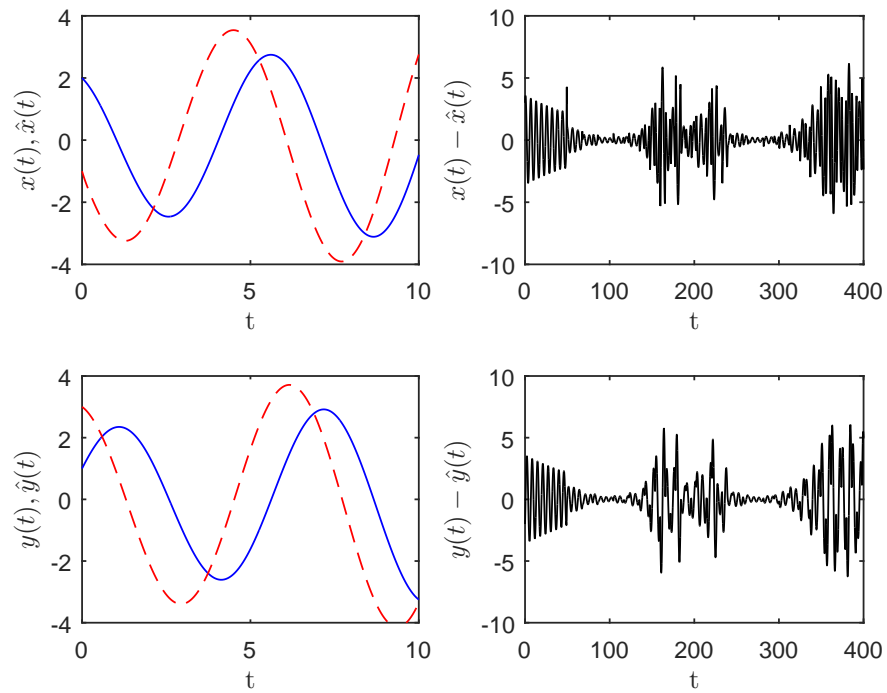
Figure 5.8: Bidirectional coupling, $d = 12$.

Figure 5.9: Unsuccessful synchronization; bidirectional coupling, $d = 0.03$.

6 CONCLUSION

The goal of this thesis was to provide a survey of the famous chaotic dynamical systems and to demonstrate a stability analysis and other currently investigated topics on a chosen chaotic model. The Rössler system, as the simplest chaotic system with only one nonlinear term, was chosen for this purposes. Besides the analysis of the stability of its equilibrium points, bifurcation of one of its parameters was studied extensively. The Rössler system was further employed in the topics of current research, i.e. the problems of stabilization and synchronization. The theoretical assumptions and results in each section were supported by numerical experiments using Matlab. The advantage was taken of certain Matlab tools, namely the ODE and DDE solvers.

Chapter 1 was devoted to the fundamental theory of the dynamical systems necessary for the stability and bifurcation analysis investigated in the next chapters. Chapter 2 was focused on the research of various chaotic systems presented in the literature. Besides the most famous models, which are the Lorenz or the Rössler system, some of the less common models, e.g. modified Van der Pol's oscillator, Sprott systems, were introduced as well. This chapter provided the evidence that chaos occurs in many dynamical systems across different fields of science.

In Chapter 3, the theoretical background from Chapter 1 was used to investigate the behaviour of the Rössler system in the neighbourhood of its equilibrium point. Particularly it was shown that the Rössler system can have either none, one or two fixed points. According to Routh–Hurwitz criterion, the case of two equilibrium points leads to one fixed point being always unstable, the second one being locally asymptotically stable for some suitable choices of system parameters. Two such choices were depicted to demonstrate the theoretical results. In further investigation, it was observed that the stability has just a local character since only a small basin of attraction of this point was found. The rest of Chapter 3 was dedicated to the bifurcation analysis of parameter c ($a = b = 0.1$). The numerical experiments provided a graphical solution of the transition from periodic behaviour to chaos. Some of the chaotic cases, e.g. cases when $c = 9, 13, 18$, and periodic cases, e.g. cases when $c = 5.5, 8, 12$, were illustrated in this part of the work. The construction of a bifurcation diagram also confirmed the results.

Chapter 4 forms the main part of this work as it deals with a problem of chaos control. Particularly, the investigation of stabilization of fixed points was presented. From the introduced methods, the emphasis was put on the time-delayed feedback control method following a general statement giving explicit conditions for the control parameters, i.e. the control gain and time delay. This statement was proven theoretically and supported by the numerical experiments, namely by stabilization of an unstable focus in 2D and one of the fixed points of the chaotic Rössler system. In case of the Rössler system, the parameters were chosen as $a = b = 0.1$, $c = 14$. With the use of the introduced statement, it was possible to find a domain of control parameters for successful stabilization of one of the fixed points of the system (the other fixed point turned out to be impossible to stabilize). The domain of control was computed and depicted together with the results of numerical experiments for several choices of suitable control parameters from the domain of control.

Finally, the last chapter was devoted to another currently studied topic, i.e. synchronization of two chaotic systems. Two chaotic Rössler systems were applied to demonstrate some of the methods of complete synchronization introduced in the literature. Namely the master-slave scheme with negative feedback control and bidirectional coupling scheme

was investigated. In both cases, complete synchronization of the trajectories was achieved as can be apparent from the provided results.

Synchronization of chaotic systems belongs among the topics of a great interest in the latest research in chaos theory. Thus, a future work could investigate the methods presented in Chapter 5 in more details. Furthermore, as the phenomenon of synchronization can be utilized in the secure communication by masking the information signal with a larger chaotic signal, this work could be further extended in the way of investigation of possible masking techniques and reliable synchronization of the transmitter and receiver systems.

REFERENCES

[1] PERKO, Lawrence. *Differential equations and dynamical systems*. 3rd ed. New York: Springer, c2001. ISBN 03-879-5116-4

[2] HIRSCH, Morris W., Stephen SMALE, Robert L. DEVANEY and Morris W. HIRSCH. *Differential equations, dynamical systems, and an introduction to chaos*. 2nd ed. San Diego, CA: Academic Press, c2004. Pure and applied mathematics (Academic Press), 60. ISBN 01-234-9703-5.

[3] HORÁK, Jiří and Ladislav KRLÍN. *Deterministický chaos a matematické modely turbulence*. Praha: Academia, 1996. ISBN 80-200-0416-5.

[4] KUZNETSOV, Yuri A. *Elements of Applied Bifurcation Theory*. 2nd ed. New York: Springer, 1998. ISBN 03-879-8382-1.

[5] MACUR, Jiří. *Úvod do teorie dynamických systémů a jejich simulace*. Brno: PC-DIR, 1995. ISBN 80-214-0698-4.

[6] ALLEN, Linda J. S.*An introduction to mathematical biology*. Upper Saddle River, NJ: Pearson/Prentice Hall, c2007. ISBN 01-303-5216-0.

[7] STROGATZ, Steven H. *Nonlinear dynamics and chaos: with applications to physics, biology, chemistry, and engineering*. Second edition. Boulder, CO: Westview Press, a member of the Perseus Books Group, 2015. ISBN 978-0-8133-4910-7.

[8] TAYLOR, Robert L.V. Attractors: Nonstrange to Chaotic. *SIAM Undergraduate Research Online* [online]. 2011, 4, 72-80 [cit. 2018-05-23]. DOI: 10.1137/10S01079X. ISSN 23277807. Available from: http://www.siam.org/students/siuro/vol4/S01079.pdf

[9] WOLF, Alan, Jack B. SWIFT, Harry L. SWINNEY and John A. VASTANO. Determining Lyapunov exponents from a time series. *Physica D: Nonlinear Phenomena* [online]. 1985, 16(3), 285-317 [cit. 2018-05-23]. DOI: 10.1016/0167-2789(85)90011-9. ISSN 01672789. Available from: https://chaos.utexas.edu/manuscripts/1085774778.pdf

[10] CENCINI, Massimo., Fabio. CECCONI and A. VULPIANI.*Chaos: from simple models to complex systems*. Hackensack, NJ: World Scientific, c2010. Series on advances in statistical mechanics, v. 17. ISBN 98-142-7765-7.

[11] KAPITANIAK, Tomasz. *Chaos for engineers: theory, applications, and control*. 2nd rev. ed. New York: Springer, c2000. ISBN 35-406-6574-9.

[12] SPROTT, Julien C. *Elegant chaos: algebraically simple chaotic flows*. New Jersey: World Scientific, c2010. ISBN 978-9812838810.

[13] LETELLIER, CHRISTOPHE and VALÉRIE MESSAGER. INFLUENCES ON OTTO E. RÖSSLER'S EARLIEST PAPER ON CHAOS. *International Journal of Bifurcation and Chaos*. 2010, **20**(11), 3585-3616. DOI: 10.1142/S0218127410027854. ISSN 0218-1274.

[14] BOUALI, SAFIEDDINE. FEEDBACK LOOP IN EXTENDED VAN DER POL'S EQUATION APPLIED TO AN ECONOMIC MODEL OF CYCLES. *International Journal of Bifurcation and Chaos* [online]. 1999, **09**(04), 745-756 [cit. 2018-05-23]. DOI: 10.1142/S0218127499000535. ISSN 0218-1274. Available from: http://booksc.org/book/37830767/b28c75

[15] ROSSI, Federico, Marcello Antonio BUDRONI, Nadia MARCHETTINI, Luisa CUTIETTA, Mauro RUSTICI and Maria Liria Turco LIVERI. Chaotic dynamics in an unstirred ferroin catalyzed Belousov–Zhabotinsky reaction. *Chemical Physics Letters* [online]. 2009, **480**(4-6), 322-326 [cit. 2018-05-23]. DOI: 10.1016/j.cplett.2009.09.018. ISSN 00092614. Available from: http://linkinghub.elsevier.com/retrieve/pii/S0009261409011087

[16] LI, Qian Shu and Rui ZHU. *Chaos to periodicity and periodicity to chaos by periodic perturbations in the Belousov–Zhabotinsky reaction* [online]. [cit. 2018-05-23]. DOI: 10.1016/S0960-0779(03)00103-6. ISBN 10.1016/S0960-0779(03)00103-6. Available from: http://linkinghub.elsevier.com/retrieve/pii/S0960077903001036

[17] GYÖRGYI, László and Richard J. FIELD. A three-variable model of deterministic chaos in the Belousov–Zhabotinsky reaction. *Nature* [online]. 1992, **355**(6363), 808-810 [cit. 2018-05-23]. DOI: 10.1038/355808a0. ISSN 0028-0836. Available from: http://booksc.org/book/10423268/472a3b

[18] STACHOWIAK, Tomasz and Toshio OKADA. *A numerical analysis of chaos in the double pendulum* [online]. 2006, **29**(2), 417-422 [cit. 2018-05-23]. DOI: 10.1016/j.chaos.2005.08.032. ISSN 09600779. Available from: http://linkinghub.elsevier.com/retrieve/pii/S0960077905006703

[19] CHEN, GUANRONG and TETSUSHI UETA. YET ANOTHER CHAOTIC ATTRACTOR*International Journal of Bifurcation and Chaos* [online]. 1999, **09**(07), 1465-1466 [cit. 2018-05-23]. DOI: 10.1142/S0218127499001024. ISBN 10.1142/S0218127499001024. Available from: http://booksc.org/book/21702350/1bfa2d

[20] GARDINI, L. Hopf bifurcations and period-doubling transitions in Rössler model *Il Nuovo Cimento B Series 11* [online]. 1985, **89**(2), 139-160 [cit. 2018-05-23]. DOI: 10.1007/BF02723543. ISSN 1826-9877. Available from: http://booksc.org/book/12460220/244416

[21] BARRIO, R., F. BLESA, A. DENA and S. SERRANO. *Qualitative and numerical analysis of the Rössler model: Bifurcations of equilibria* [online]. 2011, **62**(11), 4140-4150 [cit. 2018-05-23]. DOI: 10.1016/j.camwa.2011.09.064. ISSN 08981221. Available from: http://linkinghub.elsevier.com/retrieve/pii/S0898122111008455

[22] BARRIO, Roberto, Fernando BLESA and Sergio SERRANO. Qualitative analysis of the Rössler equations: Bifurcations of limit cycles and chaotic attractors. *Physica D: Nonlinear Phenomena* [online]. 2009, 238(13), 1087-1100 [cit. 2018-05-23]. DOI: 10.1016/j.physd.2009.03.010. ISSN 01672789. Available from: http://linkinghub.elsevier.com/retrieve/pii/S0167278909000864

[23] BUSCARINO, Arturo, L. FORTUNA and Mattia FRASCA. *Essentials of nonlinear circuit dynamics with MATLAB and laboratory experiments*. Boca Raton, 2017. ISBN 978-1-138-19813-5.

[24] SCHÖLL, E. and Heinz Georg SCHUSTER. *Handbook of chaos control*. 2nd, completely rev. and enlarged ed. Weinheim: Wiley-VCH, c2008. ISBN 978-3-527-40605-0.

[25] OTT, Edward, Celso GREBOGI and James A. YORKE. Controlling chaos. *Controlling Chaos* [online]. Elsevier, 1996, 1996, , 77-80 [cit. 2018-05-23]. DOI: 10.1016/B978-012396840-1/50032-1. ISBN 9780123968401. Available from: http://booksc.org/book/18393372/1f2e31

[26] PYRAGAS, K. Continuous control of chaos by self-controlling feedback. *Physics Letters A* [online]. 1992, **170**(6), 421-428 [cit. 2018-05-23]. DOI: 10.1016/0375-9601(92)90745-8. ISSN 03759601. Available from: http://linkinghub.elsevier.com/retrieve/pii/0375960192907458

[27] HÖVEL, Philipp. *Control of complex nonlinear systems with delay*. Heidelberg: Springer, 2010. ISBN 978-3642141096.

[28] SHAMPINE, L.F. a S. THOMPSON. Solving DDEs in Matlab. *Applied Numerical Mathematics* [online]. 2001, 37(4), 441-458 [cit. 2018-05-23]. DOI: 10.1016/S0168-9274(00)00055-6. ISSN 01689274. Available from: http://linkinghub.elsevier.com/retrieve/pii/S0168927400000556

[29] BOCCALETTI, S., J. KURTHS, G. OSIPOV, D.L. VALLADARES and C.S. ZHOU. The synchronization of chaotic systems. *Physics Reports* [online]. 2002, **366**(1-2), 1-101 [cit. 2018-05-23]. DOI: 10.1016/S0370-1573(02)00137-0. ISSN 03701573. Available from: http://linkinghub.elsevier.com/retrieve/pii/S0370157302001370

[30] PECORA, Louis M. and Thomas L. CARROLL. Synchronization in chaotic systems. *Physical Review Letters* [online]. 1990, **64**(8), 821-824 [cit. 2018-05-23]. DOI: 10.1103/PhysRevLett.64.821. ISSN 0031-9007. Available from: http://booksc.org/book/11418383/f351b4

[31] KOCAREV, L. and U. PARLITZ. General Approach for Chaotic Synchronization with Applications to Communication. *Physical Review Letters* [online]. 1995, **74**(25), 5028-5031 [cit. 2018-05-23]. DOI: 10.1103/PhysRevLett.74.5028. ISSN 0031-9007. Available from: http://booksc.org/book/18393542/9c69eb